NUMERICAL INTEGRATION OF THE QUASI-GEOSTROPHIC EQUATIONS FOR BAROTROPIC AND SIMPLE BAROCLINIC FLOWS

By J. G. Charney and N. A. Phillips

Institute for Advanced Study[1]

(Manuscript received 5 January 1953)

ABSTRACT

An n-level generalization of the $2\frac{1}{2}$-dimensional model is derived by specialization of the complete three-dimensional quasi-geostrophic equations. In the case $n = 1$, it reduces to the two-dimensional single-layer barometric model. In the case $n = 2$, it reduces to the double-layer barotropic model, or — what is shown to be mathematically equivalent—the $2\frac{1}{2}$-dimensional model. Methods of numerical integration of the 2- and $2\frac{1}{2}$-dimensional equations, and the machine requirements for such integrations, are discussed.

The results of a series of six two-dimensional and six $2\frac{1}{2}$-dimensional forecasts for 12 and 24 hours are presented. Although the $2\frac{1}{2}$-dimensional forecasts are noticeably superior to the two-dimensional forecasts, it is apparent that considerable improvement will be possible with models in which there are fewer artificial constraints. A method of integration is therefore proposed for the n-level generalization of the $2\frac{1}{2}$-dimensional model, and computation schemes are outlined for the general three-dimensional quasi-geostrophic equations. The semi-Lagrangian coordinate system with potential temperature as vertical coordinate is shown to exhibit favorable properties for machine integration.

1. Introduction

This paper continues the line of research set forth by the Meteorological Research Group at the Institute for Advanced Study (I.A.S.) in a series of publications dealing with the numerical prediction of the large-scale quasi-geostrophic motions of the atmosphere. The preceding articles presented a systematic theory of the geostrophic approximation, and applied this theory to simplified — in the main, barotropic — models.[2] It has now been possible, with the use of the I.A.S. electronic computing machine, to extend the barotropic investigations and to begin the study of baroclinic models. The results of these studies will be presented in this paper.

The computational magnitude of the forecast problem, as well as the difficulty of physical interpretation, is greatly increased by the introduction of a third spatial dimension into the motion. It may therefore be expected that mathematical and physical comprehension will be aided by the consideration of a hierarchy of models, in which the baroclinic effects are introduced successively in something like the order of their importance. Here one may proceed either by an increasing generalization of the barotropic model or by a decreasing specialization of the baroclinic model. The first procedure has been used successfully by a number of writers. Sutcliffe (1947) went beyond the barotropic model by taking into account the effect of the thermal-wind variation in the generation of vorticity. A closed system of equations embodying this effect was obtained by Charney *et al* (1950), and in simplified two-parametric form by Fjørtoft (1951), under the assumption that temperature changes are caused by horizontal advection alone. Phillips (1951) introduced a double-layer barotropic model, which did away with the advective assumption. Finally, Eady (1952) and Eliassen (1952) devised non-advective models, to which Eady has given the picturesque title "$2\frac{1}{2}$-dimensional" as they — in common with the aforementioned models — describe the motion of the atmosphere in terms of two dependent variables along each vertical. Phillips' model has the advantage that it describes a real physical process, namely the motion of two barotropic layers, but the disadvantage that it relates only indirectly to the actual atmosphere. However, it has been pointed out by Eliassen (1952) that the models of Phillips, Eady and Eliassen become mathematically equivalent with the proper interpretation of dependent variables and constant parameters.

It can be shown that the models of Phillips, Eady and Eliassen can be generalized to the case of n parameters along the vertical, or, in Eady's terminology, to $2 + [(n - 1)/n]$ dimensions.[3] The limit for large n is not the most general three-dimensional model, but is one that can be obtained from the most general model through ignoring certain effects due to the spatial variations of static stability and absolute vorticity. In the present article, a more direct derivation of the $2\frac{1}{2}$-dimensional model and its generalizations will be obtained by specialization of the general quasi-geostrophic equations. The advantages are that the nature of the assumptions and omissions is more appar-

[1] This work was cosponsored by the Office of Naval Research and the Geophysics Research Directorate, Air Force Cambridge Research Center, under contract N-6-ori-139 with the Office of Naval Research.

[2] Charney (1948, 1949); Charney and Eliassen (1949); Charney *et al* (1950); Bolin and Charney (1951).

[3] By taking n layers in Phillips' model, by integration through n sublayers in Eady's, or by considering moments to order n in Eliassen's.

ent, that the constants are automatically determined, and that the integration techniques can more easily be compared with those for the general equations.

The increase in the computational magnitude of the integration problem demands that serious attention be given to the economy of machine storage of data and of computation time. The storage requirements depend partly on the amount of real information contained in meteorological data, and partly on the accumulative effect of round-off errors; in general, more significant figures than are warranted by the accuracy of the data must be carried to avoid contamination by the round-off process. Also, for a given size of forecast area, the amount of data to be stored depends on the mesh size of the difference grid; and the mesh size, in turn, is a function of the allowable truncation error (the error due to the replacement of the [strict] differential equation by an [approximant] difference equation). Finally, both the storage requirements and the computation time depend very much on the particular method used for solving the difference equations.[4]

Since the economy problem is equally present in the barotropic model, where it can be studied with less effort, a series of auxiliary calculations, testing round-off error, truncation error and methods of integration, was performed on the barotropic model and is reported in the present article. Information gained from the barotropic calculations was utilized in devising a program for the integration of the $2\frac{1}{2}$-dimensional model. A series of six 24-hr numerical integrations was then carried out, with the I.A.S. computer, for the specially selected period 23–26 November 1950, a period in which a severe storm developed in the eastern United States. The forecasts were compared with a set of barotropic predictions for the same period. From the results, which are set forth at length in section 5, it will be seen that the $2\frac{1}{2}$-dimensional forecasts, while appreciably more accurate than the two-dimensional forecasts, and evidently comparable to the best subjective forecasts, nevertheless fail to predict the upper cyclogenesis associated with a rapidly developing surface cyclone.

Modifications of the $2\frac{1}{2}$-dimensional model have therefore been considered, but the evidence points to the need for more general models. An estimation of the storage requirements for the integration of the general quasi-geostrophic equations reveals that the integration is already within the realm of possibility for some existing computing machines, and in particular for the I.A.S. machine. It is therefore no longer academic to consider the theoretical and programmatical aspects of the three-dimensional integration problem. The program formulated for the I.A.S. computer is outlined in the last part of the present article.

[4] An article by Platzman (1952) will be found extremely helpful for understanding the role of modern computing machines in the solution of meteorological problems.

2. The $2\frac{1}{2}$-dimensional model and its generalizations

We assume that the motion is adiabatic, as well as quasi-static and quasi-geostrophic. The theory of the geostrophic approximation then leads to the following concise statement of the laws of motion (Charney, 1948): The flow is governed entirely by the laws of conservation of potential temperature and potential vorticity.[5] In the semi-Lagrangian coordinate system in which potential temperature is the vertical coordinate, the conservation of entropy becomes implicit; and, as shown by Shuman (1951), the motion is governed solely by a beautifully simple equation, expressing the conservation of potential vorticity. This equation is discussed in the last section of this article. For the present, however, it is more convenient to employ a coordinate system in which pressure is the vertical coordinate. The equations of motion in this variable have been developed systematically by Eliassen (1949).

We adopt the following notation: p is pressure, z height, ρ density, α specific volume, T absolute temperature, R the gas constant, c_v and c_p the specific heats of air at constant volume and constant pressure, respectively, θ potential temperature, f the Coriolis parameter, g the acceleration of gravity, ϕ the geopotential gz, d/dt the individual derivative, $\boldsymbol{k}$ the upward-pointing vertical unit vector, ω the individual derivative of p, $\boldsymbol{v}$ the horizontal vector velocity, and ∇ is the horizontal del-operator applied to a quantity which varies in an isobaric surface. In the p-system, the energy equation for adiabatic flow may be written

$$\frac{d \ln \theta}{dt} = \frac{\partial \ln \theta}{\partial t} + \boldsymbol{v} \cdot \nabla \ln \theta + \omega \frac{\partial \ln \theta}{\partial p} = 0, \quad (1)$$

where

$$\ln \theta = \text{constant} + (c_v/c_p) \ln p + \ln \alpha. \quad (2)$$

An approximate form of the potential vorticity equation suitable for our purposes is (Charney, 1948, eq. 47)

$$d(\eta \, \partial \ln \theta/\partial p)/dt = 0, \quad (3)$$

where η is the vertical component of absolute "isobaric" vorticity; *i.e.*,

$$\eta = \boldsymbol{k} \cdot \nabla \times \boldsymbol{v} + f. \quad (4)$$

In the evaluation of θ, $\boldsymbol{v}$ and η, we employ the hydrostatic and geostrophic relationships,

$$\partial \phi/\partial p + \alpha = 0, \quad (5)$$

and

$$\boldsymbol{v} \approx \boldsymbol{v}_g \equiv f^{-1} \boldsymbol{k} \times \nabla \phi. \quad (6)$$

Thus,

$$\eta \approx \eta_g \equiv f^{-1} \nabla \cdot \nabla \phi + f, \quad (7)$$

and

$$\ln \theta = \text{constant} + (c_v/c_p) \ln p + \ln (-\partial \phi/\partial p). \quad (8)$$

[5] The law of conservation of potential vorticity was discovered by Rossby (1940).

It will be useful to write down the equation for the vertical vorticity component,

$$d\eta_g/dt + \eta_g \nabla\cdot v + k\cdot\nabla\omega \times \partial v_g/\partial p = 0, \quad (9)$$

and the continuity equation,[6]

$$\nabla\cdot v + \partial\omega/\partial p = 0. \quad (10)$$

Using these, we see that the potential vorticity equation (3) involves the customary approximation of ignoring the conversion of horizontal to vertical vorticity, expressed by the third term in (9). Indeed, if one omits this term, (3) results from eliminating $\nabla\cdot v$ and $\partial\omega/\partial p$ between (9), (10) and

$$d(\partial \ln \theta/\partial p)/dt + (\partial\omega/\partial p)\,\partial \ln \theta/\partial p = 0, \quad (11)$$

the equation obtained by differentiating (1) with respect to p, and making use of the relationship

$$\partial v_g/\partial p\cdot\nabla \ln \theta = 0, \quad (12)$$

which follows from (6) and (8).

The change of vorticity produced by vertical advection is an effect of the same magnitude as the change produced by the turning of the vortex tubes. If we also ignore this term, and replace $\nabla\cdot v$ by $-\partial\omega/\partial p$, (9) takes the simple form

$$\eta_g^{-1} D\eta_g/Dt = \partial\omega/\partial p, \quad (13)$$

where the operator D/Dt is defined by

$$D/Dt \equiv \partial/\partial t + v_g\cdot\nabla. \quad (14)$$

Henceforth, we shall dispense with the subscript g, as it will always be understood that quantities are to be evaluated geostrophically.

A conservation equation from which the $2\frac{1}{2}$-dimensional model and its generalizations are derived is now obtained by ignoring, in addition, the vertical advection of the static stability term in (11). In place of (11), we write

$$D(\partial \ln \theta/\partial p)/Dt + (\partial\omega/\partial p)\,\partial \ln \theta/\partial p = 0. \quad (15)$$

Elimination of $\partial\omega/\partial p$ by means of (13) then gives

$$\frac{1}{\eta}\frac{D\eta}{Dt} + \left(\frac{\partial \ln \theta}{\partial p}\right)^{-1}\frac{D}{Dt}\left(\frac{\partial \ln \theta}{\partial p}\right) = 0, \quad (16)$$

or

$$D(\eta\,\partial \ln \theta/\partial p)/Dt = 0. \quad (17)$$

In view of (7) and (8), we see that the only dependent variable in the above equation is ϕ. Therefore this equation, together with the appropriate boundary conditions, suffices to determine the motion of the atmosphere.

The approximation used in deriving (15) may be given the following interpretation: We consider two adjacent unit isentropic surfaces, separated by the small pressure differential δp, and a vertical fluid cylinder of small cross-section δA, confined between the surfaces. Equations (10) and (11) state that the mass $\delta A\ \delta p$ remains constant. Hence, the horizontal divergence $(\delta A)^{-1}\,d(\delta A)/dt$ is the negative of the fractional individual derivative of δp, $(\delta p)^{-1}\,d(\delta p)/dt$. The approximation (15) then states that this fractional derivative may be calculated as though the particles moved horizontally instead of along isentropic surfaces. Now the fractional rate of change of δp — or of δA — is due to the widening or narrowing of the unit isentropic layer. If the changes in the pressure thickness of this layer were small compared to its depth, we could replace the static stability factor in (16) by its mean value for an isobaric surface. Unfortunately, this is not accurately the case. Nevertheless, to simplify matters, we shall suppose that it is. Furthermore, since the error that we make in ignoring the horizontal variation of the static stability factor is no larger than the error made in ignoring its vertical variation, we shall replace it by a constant. It could be argued that, by the same token, the factor appearing in the first term of (16) should also be replaced by a constant mean value $\bar{\eta}$. That we do not do so at this stage is primarily for formal reasons; we wish to obtain equivalence with the layered barotropic model.

The $2\frac{1}{2}$-dimensional model is derived as a special case of the following more general model. Denoting the constant value of $\partial \ln \theta/\partial p$ by $-s$, and making use of (12), we may write (16) in the form

$$D \ln \eta/Dt = s^{-1}\,\partial(D \ln \theta/Dt)/\partial p. \quad (18)$$

At the top of the atmosphere, $\omega = dp/dt = 0$; and, since there is no special reason why $\partial \ln \theta/\partial p$ should approach zero with decreasing pressure, we have from (1) that

$$\lim_{p\to 0}\omega = 0 \quad \text{or} \quad \lim_{p\to 0}\frac{D \ln \theta}{Dt} = 0. \quad (19)$$

At the ground, which we suppose level, the strict condition is that the vertical velocity shall vanish, *i.e.*, that the horizontal individual derivative of θ shall be zero. However, if we set the isobaric individual derivative equal to zero, *i.e.*, $\partial \ln \theta/\partial t = -v\cdot\nabla \ln \theta$ at $p = p_0$, the mean surface pressure, the percentage error will average less than 5 per cent. Indeed, this is one of the better meteorological approximations. Hence, we may put

$$\omega(p_0) = 0 \text{ or } (D \ln \theta/Dt)_{p=p_0} = 0. \quad (20)$$

The lateral boundary conditions will be left for later consideration.

Consider now a division of the interval $p = 0$ to $p = p_0$ into n equal subintervals, δp, and denote quantities at the midpoint of each interval by the sub-

[6] Note that we do not approximate $\nabla\cdot v$ by $\nabla\cdot v_g$. The avoidance of this pitfall is, in fact, the dynamical basis of the geostrophic approximation.

script k ($k = 1, 2, \cdots, n$) and quantities at the upper and lower end-points of each interval respectively by $k - \frac{1}{2}$ or $k + \frac{1}{2}$. If we put $k = 1$ at $p = \frac{1}{2}\,\delta p$, and $k = n$ at $p_0 - \frac{1}{2}\,\delta p$, the points $p = 0$ and $p = p_0$ correspond to $k = \frac{1}{2}$ and $k = n + \frac{1}{2}$, respectively. It is convenient to introduce the operator $\mathfrak{D}_k$, defined by

$$\mathfrak{D}_k Q \equiv Q_{k+\frac{1}{2}} - Q_{k-\frac{1}{2}} \quad \text{or} \quad \mathfrak{D}_{k-\frac{1}{2}} Q \equiv Q_k - Q_{k-1}.$$

We now write (18) for each of the points p_k, with the pressure derivative on the right-hand side replaced by a centered difference quotient. Thus,

$$(D \ln \eta/Dt)_k = (s\,\delta p)^{-1}\,\mathfrak{D}_k(D \ln \theta/Dt). \tag{21}$$

From (8), we find

$$(D \ln \theta/Dt)_{k+\frac{1}{2}} = D_{k+\frac{1}{2}}(\ln \mathfrak{D}_{k+\frac{1}{2}}\phi)/Dt, \tag{22}$$

except for $k = 0, n$. It follows that, for $k \neq 1, n$,

$$(D \ln \eta/Dt)_k = (s\,\delta p)^{-1}[D_{k+\frac{1}{2}}(\ln \mathfrak{D}_{k+\frac{1}{2}}\phi)/Dt - D_{k-\frac{1}{2}}(\ln \mathfrak{D}_{k-\frac{1}{2}}\phi)/Dt]. \tag{23}$$

Approximating ϕ_k by $\frac{1}{2}(\phi_{k+\frac{1}{2}} + \phi_{k-\frac{1}{2}})$, we find from (6) that

$$(DZ/Dt)_{k+\frac{1}{2}} = (DZ/Dt)_{k+1} = (DZ/Dt)_k,$$
$$Z = \ln(\phi_{k+1} - \phi_k). \tag{24}$$

Hence, (23) becomes, for $k \neq 1, n$,

$$\left(\frac{D \ln \eta}{Dt}\right)_k = \frac{1}{s\,\delta p}\left(\frac{D}{Dt}\right)_k \ln\left(\frac{\phi_{k+1} - \phi_k}{\phi_k - \phi_{k-1}}\right), \tag{25}$$

or

$$\left(\frac{D}{Dt}\right)_k\left[\eta_k\left(\frac{\phi_{k+1} - \phi_k}{\phi_k - \phi_{k-1}}\right)^{-\kappa}\right] = 0, \tag{26}$$

where $\kappa = (s\,\delta p)^{-1} = -(\delta p\,\partial \ln \theta/\partial p)^{-1}$.

At the levels adjacent to the ground and the top of the atmosphere, we substitute the boundary conditions (20) and (19) in (21), to obtain

$$\left(\frac{D}{Dt}\right)_1 \frac{\eta_1}{(\phi_1 - \phi_2)^{\kappa}} = 0, \tag{27}$$

and

$$\left(\frac{D}{Dt}\right)_n \frac{\eta_n}{(\phi_{n-1} - \phi_n)^{-\kappa}} = 0. \tag{28}$$

The system [(26), (27), (28)] is the required generalization of the $2\frac{1}{2}$-dimensional model. With further approximation, it can be shown to govern the motion of an atmosphere composed of n barotropic layers. We shall, however, content ourselves with showing that it can be directly related to the two-barotropic layer model, and therefore to all $2\frac{1}{2}$-dimensional models. In the process, the similarity conditions for the two-layer model will fall out.

Set $p_0 = 1000$ mb and let $n = 2$, *i.e.*, $\delta p = 500$ mb. The above system [(26), (27), (28)] then reduces to

$$\left(\frac{D}{Dt}\right)_1 \frac{\eta_1}{(\phi_1 - \phi_2)^{\kappa}} = 0, \left(\frac{D}{Dt}\right)_2 \frac{\eta_2}{(\phi_1 - \phi_2)^{-\kappa}} = 0, \tag{29}$$

where ϕ_1 is the geopotential at 250 mb and ϕ_2 the geopotential at 750 mb. The exponent κ may be written

$$\kappa = -\left(\delta p\,\frac{\partial \ln \theta}{\partial p}\right)^{-1} \approx \left(\frac{\theta_1 - \theta_2}{\theta_{1\frac{1}{2}}}\right)^{-1}, \tag{30}$$

and has approximately the value 9.

The difference $\phi_1 - \phi_2$ is proportional to the mean temperature in the layer between 750 and 250 mb. Its deviation δD ($\equiv \phi_1 - \phi_2 - D$) from its mean value D is not greater than 6 or 7 per cent. Hence, we may write, with fair approximation,

$$(\phi_1 - \phi_2)^{\kappa} \approx D^{\kappa-1}(D + \kappa\,\delta D),$$
$$(\phi_1 - \phi_2)^{-\kappa} \approx D^{-\kappa-1}(D - \kappa\,\delta D).$$

The equations of motion then become

$$\left(\frac{D}{Dt}\right)_1 \frac{\eta_1}{D + \kappa\,\delta D} = 0, \left(\frac{D}{Dt}\right)_2 \frac{\eta_2}{D - \kappa\,\delta D} = 0. \tag{31}$$

Consider now Phillips' model, an atmosphere composed of two homogeneous incompressible fluid layers of different density, confined between rigid horizontal surfaces. Let ρ' be the density of the upper fluid and ρ the density of the lower fluid. Assume that each fluid layer has the same mean depth $\frac{1}{2}H$, so that H is the total depth. Let δh be the deviation of the height of the interface from its mean value; let p' be the pressure at the upper rigid surface and p the pressure at the lower. Then, from the hydrostatic approximation, we have (apart from an irrelevant constant) $p = p' + g(\rho - \rho')\,\delta h$, or, defining $\phi = p/\rho$, $\phi' = p'/\rho'$, $\epsilon = \rho'/\rho$,

$$(1 - \epsilon)\,\delta h = z - \epsilon z'. \tag{32}$$

The equations of motion are the potential vorticity equations,

$$\frac{D}{Dt}\left(\frac{\eta}{\frac{1}{2}H + \delta h}\right) = 0, \quad \frac{D}{Dt}\left(\frac{\eta'}{\frac{1}{2}H - \delta h}\right) = 0, \tag{33}$$

where $\eta = gf^{-1}\nabla\cdot\nabla z + f$ and $\eta' = gf^{-1}\nabla\cdot\nabla z' + f$. (The operator D/Dt here applies to a horizontal surface.) Let us now identify the quantity $(1 - \epsilon)$ with $\kappa^{-1} \approx \frac{1}{9}$, so that ϵ is nearly unity. Approximately, therefore, $\delta h = \kappa(z - z')$. We see that (31) and (33) are identical. For we need only identify $z - z'$ and H by means of the equations

$$g(\tfrac{1}{2}H + \delta h) = \tfrac{1}{2}gH + \kappa g(z - z') = D + \kappa(\phi_1 - \phi_2 - D),$$

and

$$g(\tfrac{1}{2}H - \delta h) = \tfrac{1}{2}gH - \kappa g(z - z') = D - \kappa(\phi_1 - \phi_2 - D).$$

We obtain $gH = 2D$, and

$$g(z - z') = \phi_1 - \phi_2 - D.$$

The latter relation can always be satisfied by adding suitable constants to z and z', that is, by changing the

levels at which the pressure is measured in each fluid layer. Hence, we have the result that the motions of the $2\frac{1}{2}$-dimensional model, defined by (31), are identical to those in an atmosphere composed of two barotropic layers whose mean thicknesses are each equal to the mean thickness of the 750- – 250-mb layer in the atmosphere and whose density ratio is approximately 8/9.

Except for the case $n = 2$, the system [(26), (27), (28)] is unwieldy for computation. In accordance with an earlier suggestion, a simpler form is obtained by replacing the factor η in (16) by a suitable mean value $\bar{\eta}$, and by writing

$$\frac{D}{Dt}\ln\theta = \frac{D}{Dt}\ln\alpha \approx \frac{1}{\bar{\alpha}}\frac{D\alpha}{Dt} = -\frac{1}{\bar{\alpha}}\frac{D}{Dt}\frac{\partial\phi}{\partial p},$$

where $\bar{\alpha} = \bar{\alpha}(p)$ is a standard-atmosphere specific volume. An empirical justification for this simplification is given in section 5. In place of the system [(26), (27), (28)], we obtain

$$\frac{D}{Dt_k}[\eta_k + \pi_k(\phi_{k+1} - \phi_k) - \pi_{k-1}(\phi_k - \phi_{k-1})] = 0, \quad (34)$$

$$(k = 1, 2, \cdots, n),$$

where

$$\pi_k = 0 \quad \text{for} \quad k = 0, n,$$
$$\pi_k = \kappa\bar{\eta}(\bar{\alpha}_{k+\frac{1}{2}}\,\delta p)^{-1} \quad \text{for} \quad k \neq 0, n. \quad (35)$$

3. Integration of the barotropic vorticity equation

The barotropic vorticity equation is most simply derived as the finite-difference approximation to (18) for the most elementary division of the vertical scale, *i.e.*, by taking $n = 1$ in the scheme leading to the generalization of the $2\frac{1}{2}$-dimensional model. We replace the pressure derivative in (18), at the midpoint $p_0/2$ of the interval $p = 0$ to $p = p_0$, by the centered difference quotient

$$p_0^{-1}[(D\ln\theta/Dt)_{p_0=p_0} - (D\ln\theta/Dt)_{p=0}],$$

and find from (19) and (20) that it vanishes. Hence,

$$\left(\frac{D\eta}{Dt}\right)_{p=\frac{1}{2}p_0} \equiv \left(\frac{\partial\eta}{\partial t} + v\cdot\nabla\eta\right)_{p=\frac{1}{2}p_0} = 0. \quad (36)$$

To discuss this equation, we map the spherical earth conformally onto a plane and introduce a Cartesian coordinate system (x, y) in the plane. If m is the magnification factor, the del operator on the earth becomes multiplied by m in passing to the plane. Introducing the notation $\nabla^2 = \partial^2/\partial x^2 + \partial^2/\partial y^2$ for the Laplace operator in the plane and $J(\alpha, \beta) \equiv \partial(\alpha, \beta)/\partial(x, y)$ for the Jacobian of α and β, we may write (36) in the form

$$\begin{aligned}\eta &= f^{-1}m^2\nabla^2\phi + f,\\ \nabla^2(\partial\phi/\partial t) &= J(\eta, \phi),\end{aligned} \quad (37)$$

or in the form

$$\begin{aligned}\nabla^2\phi &= \xi,\\ \eta &= f^{-1}m^2\xi + f,\\ \partial\xi/\partial t &= J(\eta, \phi).\end{aligned} \quad (38)$$

The integration procedure depends essentially on whether one chooses (37) or (38) as the governing set of equations. Although the two are mathematically equivalent, they lead to different computation schemes: in the first, the history of the motion is carried by ϕ; in the second, it is carried by ξ.

Method of solution A.—The following computations, leading from time t to time $t + \Delta t$, are performed. Starting with $\phi^{t-\Delta t}$ and ϕ^t:

1. Calculate $(\partial\xi/\partial t)^t$ from the difference analogue of

$$(\partial\xi/\partial t)^t = J(f^{-1}m^2\nabla^2\phi^t + f, \phi^t); \quad (39)$$

2. Solve for $(\partial\phi/\partial t)^t$ from the difference analogue of the Poisson equation,

$$\nabla^2(\partial\phi/\partial t)^t = (\partial\xi/\partial t)^t; \quad (40)$$

3. Calculate $\phi^{t+\Delta t}$ from

$$\phi^{t+\Delta t} = \phi^{t-\Delta t} + 2\,\Delta t\,(\partial\phi/\partial t)^t. \quad (41)$$

Method of solution B.—Starting with $\xi^{t-\Delta t}$ and ξ^t:

1. Solve for ϕ^t from the difference analogue of the Poisson equation,

$$\nabla^2\phi^t = \xi^t; \quad (42)$$

2. Calculate $(\partial\xi/\partial t)^t$ from the difference analogue of

$$(\partial\xi/\partial t)^t = J(m^2f^{-1}\xi^t + f, \phi^t); \quad (43)$$

3. Calculate $\xi^{t+\Delta t}$ from

$$\xi^{t+\Delta t} = \xi^{t-\Delta t} + 2\,\Delta t\,(\partial\xi/\partial t)^t. \quad (44)$$

Procedure A was used by Charney *et al* (1950), in an article entitled "Numerical integration of the barotropic vorticity equation" and hereafter designated by the abbreviation NI. They showed that the boundary conditions on (37) or (38), for a region bounded by a simple closed curve, are: ϕ must be prescribed on the boundary for all time; η (or ξ) must be prescribed as a function of time when fluid is entering the region, but must not be prescribed when fluid is leaving the region. From the geostrophic relationship, it can be seen that influx or efflux is determined by the tangential derivative of ϕ on the boundary, taken in the proper sense, and therefore is determined by the boundary values of ϕ. The simplest condition on ϕ is that it be constant with time. For short periods of time, this rather unrealistic condition will not greatly affect the internal motion. For longer periods, a subjective forecast for the boundary could be used, or else a method which will be described in a subsequent paragraph.

The stipulation ϕ = constant implies the homogeneous condition $(\partial\phi/\partial t)^t = 0$ on the boundary for the Poisson equation (40). With this condition, and with a rectangular boundary, the Fourier transform

method is well adapted to a computer with a small variable-storage capacity, such as the *Eniac*. This method will now be briefly described.

We define a rectangular grid of points by the coordinates

$$x = i\,\Delta s,\ y = j\,\Delta s,\ (i = 0, 1, \cdots, p;\ j = 0, 1, \cdots, q),$$

and denote quantities at the point i, j by the subscript ij. In the same manner, we replace t by $\tau\,\Delta t$, so that τ has integral values. Using centered space differences, we replace the Laplacian of a quantity Q by the finite difference approximation

$$\nabla_{ij}^2 Q = (\Delta s)^{-2}(Q_{ij+1} + Q_{ij-1} + Q_{i+1j} + Q_{i-1j} - 4Q_{ij}).$$

Equation (40) becomes

$$\nabla_{ij}^2\left(\frac{\partial\phi}{\partial t}\right)^{\tau} = \left(\frac{\partial\xi}{\partial t}\right)_{ij}^{\tau}, \quad \begin{matrix}(i = 1, 2, \cdots, p-1;\\ j = 1, 2, \cdots, q-1),\end{matrix} \tag{45}$$

and the boundary conditions become

$$\left(\frac{\partial\phi}{\partial t}\right)_{0j}^{\tau} = \left(\frac{\partial\phi}{\partial t}\right)_{pj}^{\tau} = \left(\frac{\partial\phi}{\partial t}\right)_{i0}^{\tau} = \left(\frac{\partial\phi}{\partial t}\right)_{iq}^{\tau} = 0,$$
$$(i = 0, 1, \cdots, p;\ j = 0, 1, \cdots, q). \tag{46}$$

Because of the homogeneity of the boundary conditions on $\partial\phi/\partial t$, we may represent $(\partial\phi/\partial t)_{ij}^{\tau}$ by the finite sine series

$$\left(\frac{\partial\phi}{\partial t}\right)_{ij}^{\tau} = \sum_{l=1}^{p-1}\sum_{m=1}^{q-1} a_{lm}\sin\frac{\pi li}{p}\sin\frac{\pi mj}{q}, \tag{47}$$
$$(i = 1, \cdots, p-1;\ j = 1, \cdots, q-1).$$

Substitution into (45) then gives, after some reduction,

$$-4(\Delta s)^{-2}\sum_{l=1}^{p-1}\sum_{m=1}^{q-1} c_{lm}a_{lm}\sin\frac{\pi li}{p}\sin\frac{\pi mj}{q} = \left(\frac{\partial\xi}{\partial t}\right)_{ij}^{\tau}, \tag{48}$$

where $c_{lm} = \sin^2(\pi l/2p) + \sin^2(\pi m/2q)$. Multiplying by $\sin(\pi ri/p)\sin(\pi sj/k)$, and summing over i and j, we obtain

$$-4(\Delta s)^{-2}a_{rs}c_{rs} = \sum_{i=1}^{p-1}\sum_{j=1}^{q-1}\left(\frac{\partial\xi}{\partial t}\right)_{ij}^{\tau}\sin\frac{\pi ri}{p}\sin\frac{\pi sj}{q}, \tag{49}$$
$$(r = 1, \cdots, p-1;\ s = 1, \cdots, q-1),$$

from which a_{rs} is determined, and, by substitution in (47), also $(\partial\phi/\partial t)_{ij}^{\tau}$.

We note that there are two Fourier transforms of the type $\sum_{i=1}^{p-1}\alpha_{ij}\sin(\pi im/p)$, and two of the type $\sum_{j=1}^{q-1}\alpha_{ij}\sin(\pi lj/q)$, involved in the solution of the Poisson equation (45). The first type requires $(p-1)(q-1)^2$ multiplications, and the second $(p-1)^2(q-1)$ multiplications; in all, $(2p + 2q - 4)(p-1)(q-1)$ multiplications are required.

It is of interest to inquire into the machine storage-demands made by procedure A. We assume that all the initial data and all the results of intermediate calculation are stored in a readily accessible form, in what is called the "memory" of the machine. At time τ, the $2(p+1)(q+1)$ quantities $\phi_{ij}^{\tau-1}$ and ϕ_{ij}^{τ} are stored. (ξ is assumed to be zero on those parts of the boundary where influx occurs.) In stage 1, the quantity $(\partial\xi/\partial t)_{ij}^{\tau}$ is calculated point by point and stored. At the end of this stage, a total of $2(p+1)(q+1) + (p-1)(q-1)$ are stored, *i.e.*, $\phi_{ij}^{\tau-1}$, ϕ_{ij}^{τ} at all points and $(\partial\xi/\partial t)_{ij}^{\tau}$ at interior points. During stage 2, the $(\partial\xi/\partial t)$'s are systematically replaced by successive Fourier transforms, until the $(\partial\phi/\partial t)$'s are obtained. Therefore, the storage of at most one additional row or column of numbers is required. In stage 3, the $\phi^{\tau-1}$ are replaced by the ϕ^{τ}, and the ϕ^{τ} by the $\phi^{\tau+1}$ to prepare for the next time step. Finally a small number of constants and the quantities $\sin(\pi u/p)$, $\sin(\pi v/p)$ $[u = 1, \cdots, (p-1)^2;\ v = 1, \cdots, (q-1)^2]$ and $\sin^2(\pi u/2p)$, $\sin^2(\pi v/2q)$ $[u = 1, \cdots, p-1;\ v = 1, \cdots, q-1]$ must also be stored. But, from the congruence property of the sine,

$$\sin[\pi(u+p)/p] = -\sin(\pi u/p),$$

we see that, in reality, at most $2(p+q-2)$ sines of all types must be stored. Hence, if p and q are large, we are not far from the truth if we say that storage must be provided for three quantities per grid point.

In procedure B, the boundary conditions on ϕ for the difference analogue to the Poisson equation (38),

$$\nabla_{ij}^2\phi^{\tau} = \xi_{ij}^{\tau}, \tag{50}$$

are not homogeneous but that ϕ be a given function of time on the boundary. Therefore, unless we set $\phi = 0$ on the boundary — an obviously unreasonable procedure — the Fourier transform method is not conveniently applicable. As alternatives, however, there are various iterative methods which are related to the Southwell (1946) "relaxation" method, in which an approximate solution is determined by successive corrections of an initial guess. It should be mentioned that, whereas the Fourier transform yields an *exact* solution to the finite difference Poisson equation, that is, within the limits of round-off error, the iterative methods in general do not. But, if extreme accuracy is not required, this disadvantage is far outweighed by other positive advantages. The chief of these is that the iterative methods are also applicable to the elliptic partial differential equations with variable coefficients that occur in the three-dimensional models. Another is that the methods are *logically* simpler and require fewer instructions for the machine, thus taking up less memory space. Also, if too great accuracy is not required (or if the initial guess is good), few iterations are needed, and the computation is faster. However, the principal consideration that led to the choice of an iterative method was that it could also

be used for more general models, and consequently, that its application to the barotropic model could be expected to furnish valuable experience.

The "relaxation" method of Southwell is not itself well adapted to machine computation, as it involves subjective estimations that are not easily codified as instructions for the machine. The simplest of the routine methods adaptable to the machine, because of its logical simplicity, is probably Richardson's (1910). Dropping the time superscript on ϕ, we write (50) as

$$\Re\phi_{ij} \equiv \phi_{i+1j} + \phi_{i-1j} + \phi_{ij+1} + \phi_{ij-1} - 4\phi_{ij} - \Delta s^2\,\xi_{ij} = 0, \quad (51)$$

for the rectangular region $i=0,1,\cdots,p$; $j=0,1,\cdots,q$, on the boundary of which we assign fixed values of ϕ. The values of ϕ, at the νth stage of the iteration, are denoted by ϕ^{ν}_{ij}. The first guessed approximation then corresponds to $\nu = 0$. In general, $\Re\phi^{\nu}_{ij}$ will not be zero. We shall call it the residual. The Richardson process is simply to correct ϕ^{ν} by adding one-fourth the residual, *i.e.*,

$$\phi^{\nu+1}_{ij} = \phi^{\nu}_{ij} + \tfrac{1}{4}\Re\phi^{\nu}_{ij}. \quad (52)$$

This has the effect of reducing the residual at the point i, j to zero, provided one leaves undisturbed all the other ϕ^{ν}_{ij}. Thus,

$$\phi^{\nu}_{i+1j} + \phi^{\nu}_{ij+1} + \phi^{\nu}_{i-1j} + \phi^{\nu}_{ij-1} - 4(\phi^{\nu}_{ij} + \tfrac{1}{4}\Re\phi^{\nu}_{ij}) = \Re\phi^{\nu}_{ij} - \Re\phi^{\nu}_{ij} = 0. \quad (53)$$

If, however, all the ϕ's are simultaneously corrected by the formula (52), the resulting residuals $\Re\phi^{\nu+1}_{ij}$ will not be zero. However, it can be demonstrated rigorously that the ϕ's will converge to the exact solution with increasing ν.

Southwell (1946) has shown that convergence is hastened if (52) is applied pointwise rather than simultaneously, and if at the same time the factor $\frac{1}{4}$ is replaced by a judiciously selected variable quantity α greater than $\frac{1}{4}$. This is called "overrelaxation." If the grid is scanned in the same direction along successive rows, and if α is given a fixed value, the process is called by Frankel (1950) the "extrapolated Liebmann method." This method is defined by the iteration equations

$$\phi^{\nu+1}_{ij} = \phi^{\nu}_{ij} + \alpha\Re\phi^{\nu,\nu+1}_{ij}, \quad (54)$$

where the double index $\nu, \nu+1$ signifies that the index ν or $\nu+1$ is to be used, according as the subscripts are ij, $i+1j$, $ij+1$ or $i-1j$, $ij-1$. Frankel (1950) has determined the optimum value of the constant of overrelaxation α, and the corresponding convergence rate, as follows. The errors $\mathrm{E}^{\nu}_{ij} \equiv \phi^{\nu}_{ij} - \phi_{ij}$ satisfy the homogeneous equation corresponding to (51). We write, symbolically,

$$\mathrm{E}^{\nu+1} = \mathfrak{K}(\alpha)\,\mathrm{E}^{\nu}, \quad (55)$$

where $\mathfrak{K}(\alpha)$ is a linear operator depending on α. We expand E^{ν}_{ij} in the eigenfunctions of the operator $\mathfrak{K}$, subject to the boundary conditions on E^{ν}_{ij}. (These are that $\mathrm{E}^{\nu}_{ij} \equiv 0$ on the boundary.) Then it can be shown that, if $\mathrm{E}_{ij;r,s}$ $(r = 1,\cdots,p-1;\ s = 1,\cdots,q-1)$ are the eigenfunctions of E^{0}_{ij}, so that

$$\mathrm{E}^{0}_{ij} = \sum_{r,s} a_{rs}\,\mathrm{E}_{ij;rs},$$

and if K_{rs} are the corresponding eigenvalues, then

$$\mathrm{E}^{\nu}_{ij} = \sum_{r,s} a_{rs}(K_{rs})^{\nu}\mathrm{E}_{ij;rs},$$

where the notation $(K_{rs})^{\nu}$ means K_{rs} raised to the νth power. Frankel shows that α can be chosen so that $|K_{rs}| < 1$. Hence, the process converges. The optimum value of α is that which minimizes the maximum $|K_{rs}|$. If $\cos\beta \equiv \frac{1}{2}[\cos(\pi/p) + \cos(\pi/q)]$, the optimum value of α is $\frac{1}{2}(1+\sin\beta)^{-1}$, and the maximum absolute value of K_{rs} is $4\alpha - 1$. If p and q are large, the maximum $|K_{rs}|$ is approximately given by

$$|K_{rs}|_{\max} \approx 1 - [2\pi^2(p^{-2}+q^{-2})]^{\frac{1}{2}}.$$

In the Richardson method, the corresponding maximum $|K_{rs}|$ is given by

$$|K_{rs}|_{\max} \approx 1 - \tfrac{1}{4}\pi^2(p^{-2}+q^{-2})$$

for large p and q. It may be seen that the extrapolated Liebmann process converges faster ultimately. However, in the first few iterations the size of the residuals depends on the initial error distribution. Actually, a value of α lying between Frankel's and Richardson's was found to give the most rapid early convergence.

As many steps in the iteration process are performed as are needed to reduce the absolute value of each residual below a certain prescribed value. The number of iterations will therefore depend on the accuracy of the initial approximation. In procedure B, an obvious initial approximation is the value of ϕ_{ij} at the previous time step. A better one might be to extrapolate linearly from the preceding two time steps. However, the latter requires additional storage, namely of the penultimate ϕ.

Another iterative method has been proposed by Fjørtoft (1952), for solving equations of the type (51). In its simplest form, it is the following. Denote the quantity $\frac{1}{4}(\phi_{i+1j} + \phi_{ij+1} + \phi_{i-1j} + \phi_{ij-1})$ by $\mathfrak{K}\phi_{ij}$, so that (51) may be written symbolically as

$$(1 - \mathfrak{K})\phi_{ij} = -\tfrac{1}{4}\Delta s^2\,\xi_{ij} \equiv X_{ij}. \quad (56)$$

Formal inversion of the operator $1 - \mathfrak{K}$ gives

$$\phi_{ij} = (1-\mathfrak{K})^{-1}X_{ij} = (1 - \mathfrak{K} + \mathfrak{K}^2 - \mathfrak{K}^3 + \cdots)X_{ij}. \quad (57)$$

This formal process is then justified. Defining

$$\phi^{\nu}_{ij} = [1 - \mathfrak{K} + \cdots (-1)^{\nu-1}\mathfrak{K}^{\nu-1}]X_{ij}, \quad (58)$$

Fjørtoft shows that ϕ^{ν}_{ij} converges to ϕ_{ij} as ν tends toward infinity.

The process is, however, not different from Richardson's, for, as can be easily verified, the ϕ_{ij}^{ν} defined by (58) satisfy (52), and complete equivalence between (52) and (57) is brought about by setting $\phi_{ij}^{0} \equiv 0$.

Extensions of the above method by Fjørtoft were found to give more rapid convergence and to be well adapted to hand computation. However, they involve varying grid sizes and are therefore not suitable for machine computation.

It was shown in NI that the choice of the space and time increments, Δs and Δt, is restricted by the computational stability criterion

$$\Delta s/\Delta t \geq \sqrt{2} m |v|_{\max}, \tag{59}$$

where $|v|_{\max}$ is the maximum particle speed in the forecast region. This criterion must be satisfied if small perturbations, which are inevitably distorted, are not to amplify destructively. The ratio $\Delta s/\Delta t$ called for does not, however, correspond to the optimum ratio demanded by considerations of truncation error. The increments Δs and Δt should be chosen so as to give the same definition of the field of motion along the time axis as along the space axis. That is to say, the time truncation error and the space truncation error should be about the same. Nothing is gained if the increment of one independent variable is chosen so small that the truncation error in this variable is small, as long as the truncation error in the other variable remains large. But this requires that the ratio $\Delta s/\Delta t$ should be equal to the local speed of propagation of the flow pattern — not the local particle velocity. We should take

$$\Delta s/\Delta t \approx \sqrt{2} mc, \tag{60}$$

where c is a typical speed of displacement of the flow patterns. At the 500-mb level, $|v|_{\max}$ may be 50 m/sec or more, whereas a typical c is at most 20 m/sec. Hence, the Δt called for by the criterion (59) is perhaps two or three times too small. The computation will therefore take two or three times as long as it would if (59) did not have to be satisfied.

There appears to be a way out of the difficulty. From the point of view of computational stability, (36) behaves purely as an advective equation when Δs is sufficiently small, *i.e.*, as though $v = f^{-1}k \times \nabla\phi$ were a fixed function of space. It does not matter that η is itself a function of derivatives of ϕ. Hence, in using the method of integration B, the stability criterion (59) applies only to (43) and (44), and not to (42). This suggests that a new field of ϕ need not be calculated from ξ at the end of each time step. If, for example, Δt is required by (59) to be one hour, we may advect the vorticities for two or three one-hour steps, while holding ϕ fixed as a function of time, and only after the second or third step redetermine a new field of ϕ, and therefore of velocity. Thus, the solution of the Poisson equation (42) (which is ordinarily the most lengthy operation) need be performed only as often as is required by considerations of truncation error.

The above method cannot be employed with procedure A, because in this system it is ϕ and not η (or ξ) that carries the history of the motion; ϕ must here be determined for each time step.

We now describe the actual procedure used in obtaining a series of 24-hr barotropic forecasts.

Forecasts were desired for an overall area of 5400 by 5400 km, with an interior region of validity of about 3300 by 3300 km lying almost entirely between the 30th and 60th parallels. For an area of this size, the Lambert conformal map projection with standard parallels at 30 and 60 deg is particularly well-suited, since it distorts distances between these latitudes by less than 3.5 per cent.

If φ is latitude, R_e the radius of the earth, ρ the polar distance on the map, and ρ_E the distance from pole to equator on the map, the following relations obtain for the Lambert projection:

$$\rho^2 = \rho_E^2[(1 - \sin\varphi)/(1 + \sin\varphi)]^h, \tag{61}$$

and

$$m^2 = h^2\rho^2(R_e^2 \cos^2\varphi)^{-1}, \tag{62}$$

where h is a numerical constant (actually a function of the standard latitudes) with the value 0.71556. Defining $u \equiv (\rho/\rho_E)^2$, we have

$$\sin\varphi = (1 - u^{1/h})(1 + u^{1/h})^{-1}, \tag{63}$$

and

$$m^2 = h^2\rho^2 R_e^{-2}(1 - \sin^2\varphi)^{-1}. \tag{64}$$

In practice, $\sin\varphi$ is sufficiently well approximated between 30 and 60 deg by the linear function of u,

$$\sin\varphi = 1.056 - 1.233\,u, \tag{65}$$

and m^2 is thereafter determined from (64). The error in $\sin\varphi$ is less than 1.0 per cent, while the error in m^2 does not exceed 2.0 per cent.

The mesh size Δs used in the *Eniac* computations (NI), 628.5 km at 45°N, was definitely too large. This became very evident when forecasts made both with the stereographic and the Mercator projections were compared. The mesh size for the Mercator projection corresponded nearly to the same distance on the earth at 40 deg as the stereographic projection, but to only half the distance at 60 deg. At the latter latitude, the forecasts differed considerably; the intensity of the 12-hr 500-mb height-change areas was, on the average, some 50 per cent higher for the forecast made with the Mercator projection. Since the truncation error incurred in approximating a first derivative by a centered finite difference is proportional to the square of the increment of the

independent variable, the error would be reduced to less than $\frac{1}{4}$ its value if this distance were 300 km.

The magnitude of the error may be estimated from the Taylor's series expansions of $f(x + \Delta s)$ and $f(x - \Delta s)$. We find

$$\frac{1}{f'(x)}\left[\frac{f(x+\Delta s) - f(x-\Delta s)}{2\,\Delta s} - f'(x)\right] \approx \frac{\Delta s^2}{12}\frac{f'''(x)}{f'(x)} + O(\Delta s^4).$$

Let $f = \cos(2\pi x/L)$. Then $|f'''/f'| = 4\pi^2 L^{-2}$, and

$$\frac{\Delta s^2}{12}\frac{f'''}{f'} = \frac{\pi^2}{3}\left(\frac{\Delta s}{L}\right)^2.$$

Take $L = 2000$ km, corresponding to a motion of relatively small scale. For this wavelength, the percentage error with $\Delta s = 300$ km is 7.5 per cent, whereas with $\Delta s = 628.5$ km it is 40 per cent.

To use an increment smaller than 300 km would seem to give undue prominence to the small-scale motions, which are not governed by the geostrophic approximation and which it is our desire to smooth. Moreover, since the grid values are determined by subjective interpolation, decreasing the size of the grid interval would exaggerate errors of interpolation. The value 300 km was therefore chosen.

The corresponding value of Δt was determined by the stability condition (59). The maximum particle speed at 500 mb, for the flows investigated, was estimated to be 50 m/sec. This led to a maximum value for Δt of 1 hr and 11 min. The actual choice for Δt was 1 hour.

We may now describe in greater detail the stages in procedure B.

1. With $\xi_{ij}^{\tau-1}$ and ξ_{ij}^{τ} stored for all grid points, except for boundary points at which there is outflow, (51) is solved for ϕ_{ij}^{τ} by means of the iteration equation (54), with use of $\phi_{ij}^{\tau-1}$ as the initial guess. The constant α is determined from (55).

2. $(\partial\xi/\partial t)_{ij}^{\tau}$ is found from

$$\left(\frac{\partial \xi}{\partial t}\right)_{ij}^{\tau} = (2\,\Delta s)^{-2}[(\eta_{i+1j}^{\tau} - \eta_{i-1j}^{\tau})(\phi_{ij+1}^{\tau} - \phi_{ij-1}^{\tau}) - (\eta_{ij+1}^{\tau} - \eta_{ij-1}^{\tau})(\phi_{i+1j}^{\tau} - \phi_{i-1j}^{\tau})], \tag{66}$$

where

$$\eta_{ij}^{\tau} = m_{ij}^2 f_{ij}^{-1}\xi_{ij}^{\tau} + f_{ij}. \tag{67}$$

The quantities f_{ij} and m_{ij} are evaluated from (65) and (64). The relevant quantity here is $u = (\rho/\rho_E)^2$. This may be written

$$u = \rho_E^{-2}(\Delta s)^2[(i_p - i)^2 + (j_p - j)^2], \tag{68}$$

where the pole is given the integral coordinates i_p and j_p.

At boundary points with inflow (inflow or outflow is determined by differencing the ϕ_{ij} on the boundary adjoining the boundary point in question), ξ^{τ} is set equal to its initial value ξ^0. At boundary points with outflow, non-centered differences must be used to evaluate $(\partial\xi/\partial t)^{\tau}$.

3. At interior points, $\xi_{ij}^{\tau+1}$ is obtained from

$$\xi_{ij}^{\tau+1} = \xi_{ij}^{\tau-1} + \epsilon(\tau)\,\Delta t\,(\partial\xi/\partial t)_{ij}^{\tau}. \tag{69}$$

At $\tau = 0$, it is necessary to employ non-centered differences, that is, to set $\xi_{ij}^{\tau-1} \equiv \xi_{ij}^{0}$ and $\epsilon(0) = 1$. At all other times, $\epsilon(\tau)$ is set equal to 2. At outflow points, also, ξ_{ij}^{τ} must be used in place of $\xi_{ij}^{\tau-1}$ with $\epsilon(\tau) \equiv 1$.

By taking $\phi(i, j, \tau) \equiv \phi(i, j, 0)$ on the boundary, though this does not affect the motion at some distance from the boundary for short forecast periods, we do not use a simple property of atmosphere motion, namely that systems in middle latitudes generally move from west to east. The first tool of the forecaster, that of extrapolation, may be incorporated into the numerical forecast in the following elementary way. Suppose that the average movement of the systems is from west to east, with constant angular velocity $\dot{\lambda}$ about the polar axis. The value of $\dot{\lambda}$ is determined from past displacements.

Let us describe the motion in a coordinate system moving relative to the earth, with the same angular velocity $\dot{\lambda}$. The assumption $\phi(i, j, \tau) \equiv \phi(i, j, 0)$ is obviously better in this coordinate system. The absolute vorticity$_a$ in this system will be equal to the absolute vorticity referred to a system fixed in the earth, plus the small additional vorticity $2\dot{\lambda}\sin\varphi$, which is quite insignificant since $\dot{\lambda}$ is very small compared to Ω, the angular velocity of the earth. The velocities will be different, but, as they are calculated from the vorticities and the boundary ϕ's, it is only necessary to consider the transformation of the latter quantities. The velocity $\boldsymbol{v}'$ in the moving system may be written

$$\boldsymbol{v}' = \boldsymbol{v} - \dot{\lambda}R_e\cos\varphi\,\boldsymbol{i},$$

where $\boldsymbol{i}$ is a unit vector pointing from west to east. Hence we have only to set

$$\phi' = \phi + \dot{\lambda}\Omega R_e^2\sin^2\varphi, \tag{70}$$

on the boundaries.

We come now to a consideration of problems of storage and of computation time. The storage problem is not critical for the barotropic model, but rapidly becomes so for baroclinic models. Preliminary studies with the barotropic model will therefore aid in deciding the feasibility of baroclinic computations. The computation time is again not a factor in the barotropic integration problem, but is very much a factor in the baroclinic case, particularly if the aim is to develop practicable methods for service forecasting. Also, on purely scientific grounds, a large number of numerical forecasts will be needed to collect the inductive evidence on which general laws of atmospheric motion can be founded. The value of a numerical forecast would be greatly reduced if an excessive time were required for its preparation.

Clearly, the storage of data depends on the amount of digital significance in the data themselves. Thus, the 500-mb height used in the barotropic forecast varies by perhaps 3500 ft over the forecast area, and

is probably not more accurate than to within 50 ft. Hence, the accuracy is one part in seventy, and two decimal places should suffice for storing the height if expressed as a deviation from a standard or a synoptically averaged value. Many modern computers, including the I.A.S. machine, store and compute in the binary system, in which the base is 2 instead of 10 as in the decimal system. Seven binary places, giving an accuracy of one part in $2^7 = 128$, are therefore needed in this system.

Actually, in the course of computation, more than seven digits must be stored to allow for contamination by round-off errors. Whenever a number is stored to n places, it is rounded off .This produces a fractional error that lies between $2^{-(n+1)}$ and $-2^{-(n+1)}$. If the process during which the number is stored is repeated m times, the probable error will be increased by the factor $m^{\frac{1}{2}}$, provided the round-off errors are random.

Round-off errors in ϕ and ξ also enter indirectly, as for example in affecting the accuracy of $(\partial\xi/\partial t)_{ij}^{\tau}$ in (66), which in turn affects the accuracy of $\xi_{ij}^{\tau+1}$ in (69), and therefore again of $\phi_{ij}^{\tau+1}$ obtained from the Poisson equation (51) for time $\tau + 1$. It should be pointed out that, when an iterative process (*e.g.*, the extrapolated Liebmann) is used to solve (51), the error in ϕ is not only caused by round-off *per se*, but is also a function of the accuracy with which the final iterated solution satisfies (51). The ϕ's were stored in the machine as scaled quantities $\hat{\phi}$, such that $1 > \hat{\phi} > 0$, and $d\phi/d\hat{\phi} \approx g \times 3500$ ft. The iteration process was stopped when $|\hat{\phi}^{\nu+1} - \hat{\phi}^{\nu}| < \delta$ for all i and j, or by (54), when $|\mathcal{R}\hat{\phi}_{ij}^{\nu,\nu+1}| < \delta/\alpha$. [If $\delta = 2^{-N}$, the successive guesses for $\hat{\phi}$ must be stored to at least $N + 2$ places, if the pure round-off error incurred in *storing* $\hat{\phi}^{\nu}$ is not to interfere greatly with the convergence of (54).]

To calculate the resultant effect of these errors *ab initio* is a difficult, if not impossible, task. Accordingly, a short series of 12- and 24-hr numerical integrations were performed, with varying digital significance for the ϕ's and ξ's. A basic forecast was first obtained with $\delta = 2^{-14}$ and ξ stored to twenty places, and this was then compared to forecasts from the same initial data where δ was gradually increased to 2^{-8} and the storage of ξ decreased to 14 binary places. It was found that the error in ϕ at the end of 24 one-hour time steps remained negligible in comparison with the error of observation until δ became greater than 2^{-9}. On the basis of these experiments, twelve places for ϕ ($\delta = 2^{-10}$) and 14 for each ξ were decided upon. (It later developed that fewer places, at least as few as ten, can be used for ξ. Thus, an accuracy of approximately one part in a thousand was found sufficient for both ϕ and ξ.)

In the I.A.S. machine, information is taken out of the memory (or stored therein) in groups of forty binary digits, each such group being called a "word." Thus, one word sufficed for the three quantities ϕ^{τ}, ξ^{τ} and $\xi^{\tau-1}$ that were stored for each grid point. In the present case, the grid consisted of $19 \times 19 = 361$ points. Hence, 361 words sufficed for the storage of these quantities. We may add that approximately 300 additional words were needed for storage of intermediate results of computation, constants, and instructions to the machine. The I.A.S. machine has an electronic memory for 1024 words.

For a given forecast area, the storage depends also on the size of the finite-difference intervals, and these are determined by the allowable truncation error. Unfortunately, space truncation errors are difficult to assess as long as one is dealing with flows that are determined initially only at a discrete set of observation points. The errors of interpolation cannot here be separated from the truncation errors. This difficulty could be partially overcome, if one had a mathematically exact knowledge of the evolution of a flow pattern closely resembling the motion in the atmosphere. The flow most nearly satisfying this condition is the finite-amplitude wave model of Craig (1945), Neamtan (1946), Thompson (1948), and Höiland (1950). Platzman[7] has given an exact solution for the corresponding difference equations. For the present, however, we have assumed that the value of 300 km for Δs is not far from optimum.

As for the time-truncation error, we have the evidence from the *Eniac* calculations (NI) that increasing the time interval from one to two and then three hours produced no appreciable change in a 24-hr forecast. The computation proved stable for even the 3-hr interval because the space increment was over twice its present value and the particle speeds were lower than 50 m/sec. In the present case, integrations were performed for $\Delta t = 1$, $\frac{4}{3}$ and 2 hr, to test the application of the stability criterion. Instability manifests itself by the exponential growth of small disturbances in the field of geopotential or vorticity. Their rate of amplification can be estimated from the theory presented in NI. One obtains the result that the maximum amplification factor, after n time steps, is $e^{n\theta}$, where $\theta = \text{arc cosh}\,[\sqrt{2}m\,|v|_{\max}\Delta t/\Delta s]$. In the example tested, instability was observed for $\Delta t = \frac{4}{3}$ hr and $\Delta t = 2$ hr. In the case $\Delta t = \frac{4}{3}$ hr, θ was determined from the rate of growth of small deviations from the computation for $\Delta t = 1$ hr (which was stable). With use of this value of θ, the corresponding value for the case $\Delta t = 2$ hr and the number of time steps required for the amplitude of a given perturbation to increase by a certain amount were computed and were found to agree with observation.

As previously observed, the computational stability condition permits the advection of vorticity for several (n) time steps in a velocity field that is held stationary

[7] Unpublished work.

during this period. The velocity field is redetermined by (51) only at the end of the period. Let us use the notation "nJ/L" — n Jacobian operations per extrapolated Liebmann operation — to denote this procedure. Two experiments were made to test its accuracy. These consisted in the preparation of two 12-hr forecasts, the first by means of the $2J/L$ procedure and the second by means of the $3J/L$ procedure. These forecasts were then compared with the $1J/L$ 12-hr forecast from the same data. In all these forecasts, Δt remained 1 hr. Although both the $2J/L$ and $3J/L$ forecasts were stable, their deviations from the $1J/L$ forecast were too large to warrant continued use of the process. Fig. 1 shows the difference in the 12-hr forecasts obtained by the $3J/L$ and $1J/L$ processes, together with the 12-hr changes predicted by the latter. The initial map from which the forecasts were made is shown in fig. 5. The error is due to a too-rapid northward displacement of the cyclonic vorticities associated with the deep cyclone in fig. 4. It is of just the same kind as the error produced in the position of a fluid particle in a nonstationary flow, when the mistake is made of identifying a streamline with the path. The velocity field is here attached to the vorticity field and moves with it. (Fig. 2 shows the corresponding phenomenon for a baroclinic forecast.)

The following scheme, involving the storage of four quantities per grid point, has been found to eliminate the error and to decrease the computation time. At time τ, suppose we have the quantities $\phi^{\tau-n}$, ϕ^{τ}, $\xi^{\tau-1}$ and ξ^{τ} stored. In the first step, $\xi^{\tau+1}$ is calculated from (66) and (69); the quantities $\xi^{\tau-1}$ are replaced by ξ^{τ} in the memory, and ξ^{τ} is replaced by $\xi^{\tau+1}$. The value of $\phi^{\tau+1}$ is then determined not by solution of the Poisson equation (51), but by linear extrapolation from $\phi^{\tau-n}$ and ϕ^{τ}. With the aid of this new value, $\xi^{\tau+2}$ is calculated, and a $\phi^{\tau+2}$ is determined again by extrapolation from $\phi^{\tau-n}$ and ϕ^{τ}. The whole process is carried out n times, until

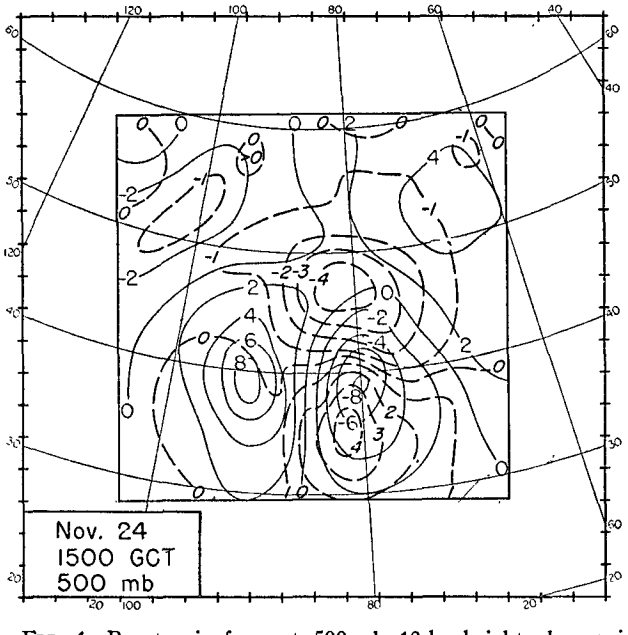

FIG. 1. Barotropic forecast 500-mb 12-hr height change in hundreds of feet. Continuous lines show forecast change when velocity field was redetermined at each time step ($1J/L$). Dashed lines show deviation from above change when velocity field was redetermined after every third time step ($3J/L$). Initial data in both cases were for 1500 GCT 24 November 1950.

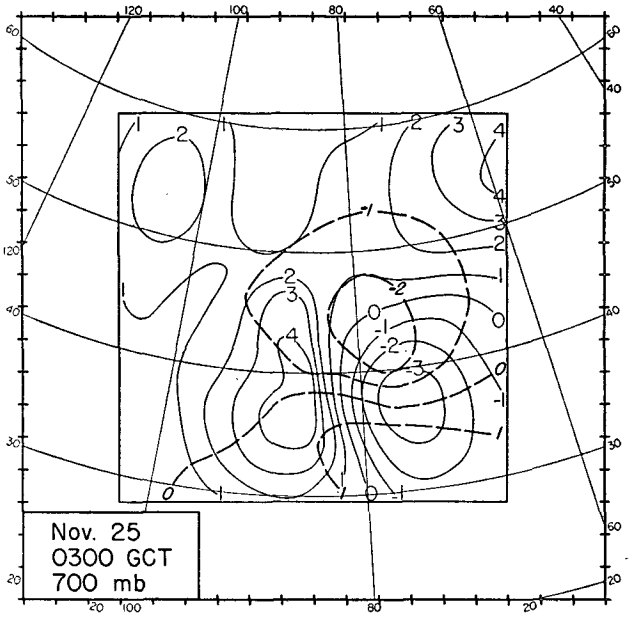

FIG. 2. Baroclinic forecast 700-mb 12-hr height change in hundreds of feet. Continuous lines show forecast change when velocity field was redetermined at each time step ($1J/L$). Dashed lines show deviation from above change when velocity field was redetermined after every third time step ($3J/L$). Initial data in both cases were for 0300 GCT 25 November 1950.

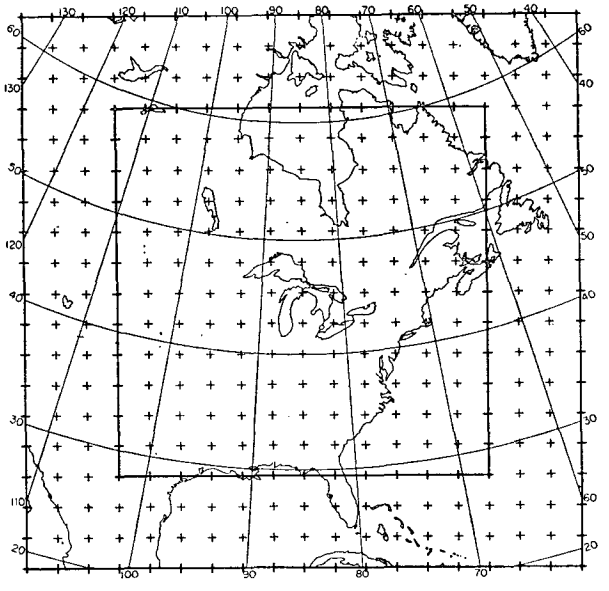

FIG. 3. Location of finite-difference lattice used in barotropic and $2\frac{1}{2}$-dimensional forecasts. Large square outlines 19 × 19 grid used for computations; smaller square outlines region over which verification was made.

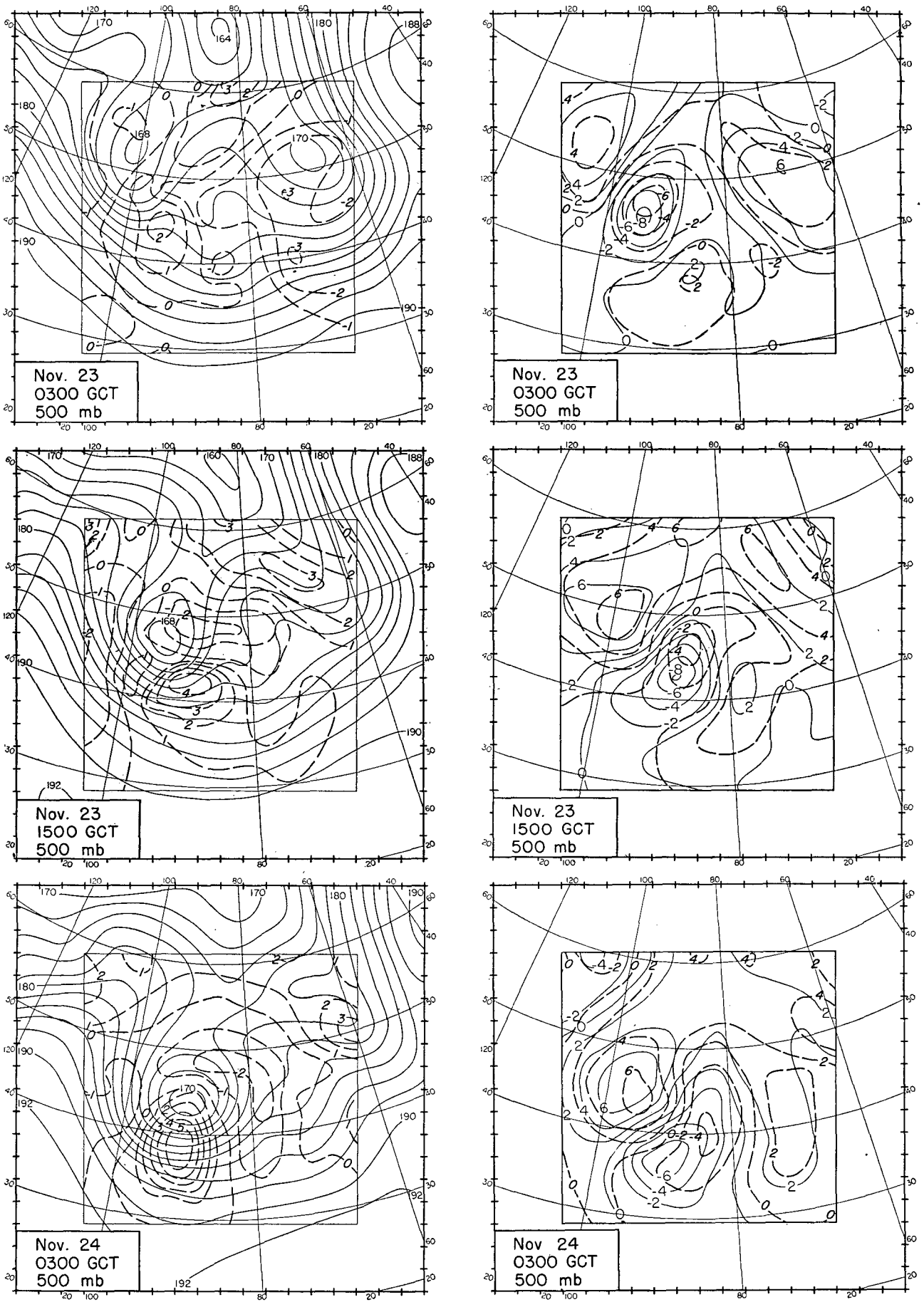

FIG. 4. 12-hr barotropic forecast data for 500-mb, November 1950. Left-hand charts contain initial 500-mb maps, with height contours (continuous lines) at 200-ft intervals for 0300 GCT on 23rd (a, top), 1500 GCT on 23rd (b, center), and 0300 GCT on 24th (c, bottom). Dashed lines on these three charts show error (forecast minus observed in hundreds of feet) in 12-hr forecast made from each initial map. Right-hand charts contain observed (continuous lines) and forecast (dashed lines) height changes (in hundreds of feet) for 12-hr period following time of corresponding chart on left.

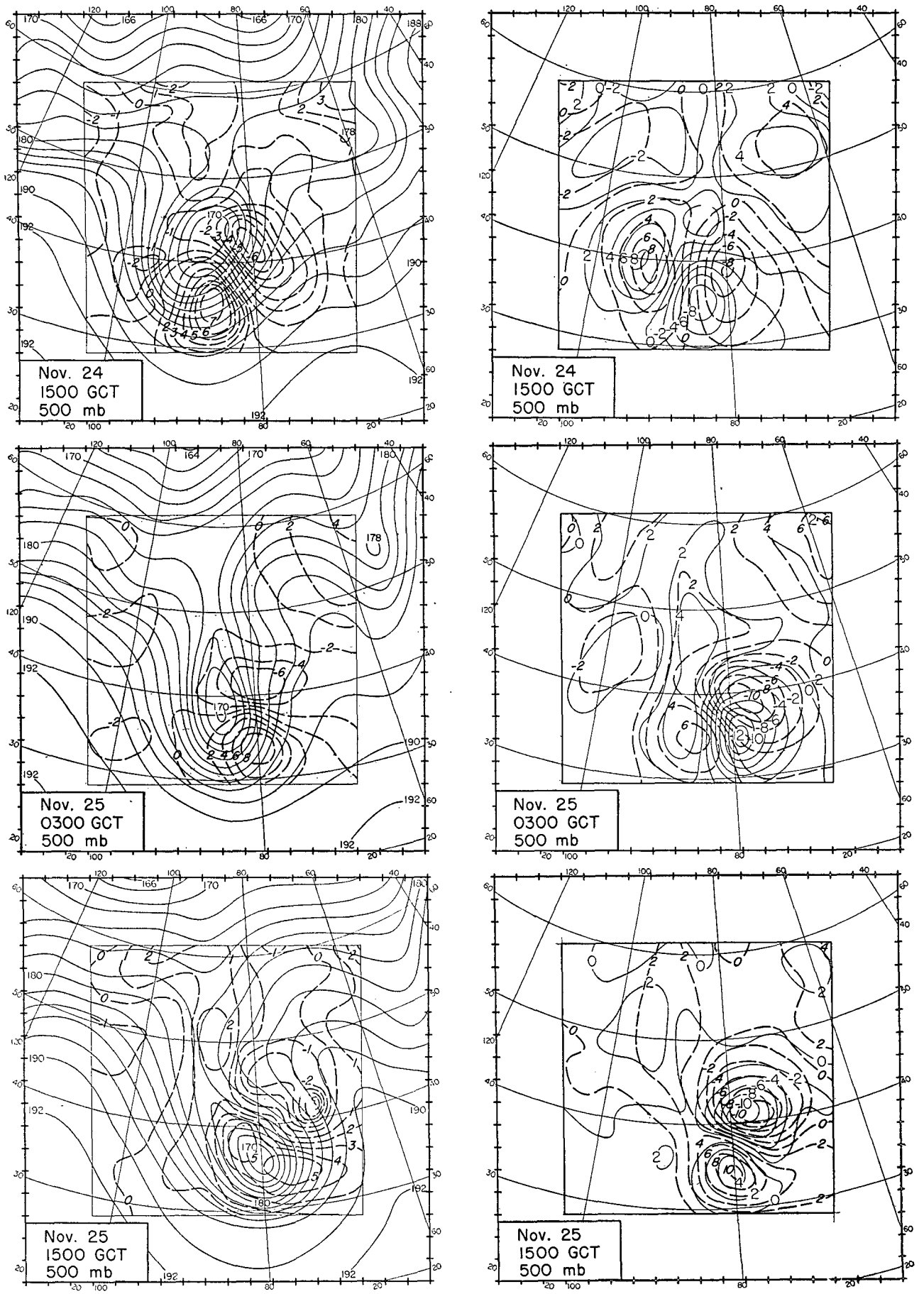

FIG. 5. 12-hr barotropic forecast data for 500 mb: (a, top), 1500 GCT 24 November 1950; (b, center), 0300 GCT 25 November 1950; (c, bottom), 1500 GCT 25 November 1950. (Refer to fig. 4 for further explanation.)

the quantities $\phi^{\tau-n}$, ϕ^{τ}, $\xi^{\tau+n-1}$ and $\xi^{\tau+n}$ are held in the memory. At this stage, $\phi^{\tau-n}$ is replaced by ϕ^{τ}, and $\phi^{\tau+n}$ is determined from $\xi^{\tau+n}$ by the solution of the Poisson equation. The induction is then complete. Initially it is necessary to advance in single time steps, until n steps have been taken. Only then do we have two quantities for the extrapolation, namely ϕ^0 and ϕ^n, and are ready to begin the induction.

The above considerations suggest an improvement of procedure B, in which a new ϕ is computed at every time step from each new ξ. Assuming that it is possible to store four quantities per grid point, we suppose that $\phi^{\tau-2}$ is stored in addition to $\phi^{\tau-1}$, $\xi^{\tau-1}$ and ξ^{τ} at the stage just preceding the calculation of ϕ^{τ} from ξ^{τ}. Instead of taking $\phi^{\tau-1}$ as the initial guess in the iterative process, we extrapolate linearly from $\phi^{\tau-2}$ and take instead $2\phi^{\tau-1} - \phi^{\tau-2}$. The initial error is thereby considerably reduced, and fewer iterations are required to reduce the residual below a prescribed value.

It is of interest to compare the computation times for different methods of integrating the barotropic equations. With procedure B, a time interval of one hour, and a rectangular grid of $19 \times 19 = 361$ points, the I.A.S. computer produced a 24-hr forecast in 48 min, at full speed. (Actually the machine operated at half-speed most of the time, and therefore required 96 min.) In each step, the machine performed 64,000 multiplications, 4,200 divisions, 314,000 additions and subtractions, and executed 1,467,000 additional orders. Of the 64,000 multiplications, 52,000 were used in solving the Poisson equation and 12,000 in computing the Jacobian. With the ϕ's stored as numbers smaller than 1, approximately 13 iterations of the extrapolated Liebmann process were required to reduce the quantity $|\hat{\phi}^{\nu+1} - \hat{\phi}^{\nu}|$ below 2^{-10}. Altogether, six-fold more time was spent in the Poisson part of the calculation than in the Jacobian part. However, it has been found that use of the modified procedure B presented in the previous paragraph, combined with a more thorough rationalization of the remainder of the code, leads to a computation time, at full speed, of about 24 min for a 24-hr forecast. With this improvement, the Poisson part of the computation consumes no more time than the Jacobian part. (*Note added in proof:* The computation time has recently been reduced to 6 min.)

It has been pointed out that the Fourier transform method (procedure A) uses approximately $2(p + q - 2)(p - 1)(q - 1)$ multiplications in the solution of the Poisson equation. With $p = q = 18$, this gives about 20,000 multiplications, as compared with approximately 52,000 in procedure B. Nevertheless, with use of procedure A, it is estimated that a computing time of at least one hour at full speed on the machine is required for a 24-hr forecast in one-hour steps. This is because of the large number of non-arithmetical or "logical" orders the machine is required to execute.

4. Integration of the $2\frac{1}{2}$-dimensional equations

As in the treatment of the barotropic model, we introduce a Lambert conformal mapping and a Cartesian system of coordinates x, y in the conformal plane. With the notation $\phi_2 \equiv \phi$, $\phi_1 \equiv \phi'$, $\eta_2 \equiv \eta$, $\eta_1 \equiv \eta'$, (31) becomes

$$\partial q/\partial t = m^2 f^{-1} J(q, \phi), \tag{71}$$

and

$$\partial q'/\partial t = m^2 f^{-1} J(q', \phi'), \tag{72}$$

where

$$q = [m^2 f^{-1} \nabla^2 \phi + f][(\kappa + 1)D - \kappa(\phi' - \phi)]^{-1}, \tag{73}$$

and

$$q' = [m^2 f^{-1} \nabla^2 \phi' + f][\kappa(\phi' - \phi) - (\kappa - 1)D]^{-1}. \tag{74}$$

From the manner in which (29) was derived, it is seen that ϕ' is the geopotential of the 250-mb surface and ϕ is the geopotential of the 750-mb surface. Since these are not standard surfaces, it is inconvenient to determine their heights from radiosonde reports. However, because of the crude manner in which the vertical scale of motion is being treated, there is no difficulty in deriving an equivalent set of equations which apply at the standard levels, 300 and 700 mb. This is done by using approximations that are already implicit in the derivation of (29). Thus, if we write (13) for the 300- and 700-mb levels, and in each case evaluate the vertical derivative by using centered differences and a vertical increment $\delta p = 600$ mb, we find, in view of conditions (19) and (20),

$$\frac{1}{\eta_3}\left(\frac{D\eta}{Dt}\right)_3 = \frac{\omega_6}{\delta p}; \quad \frac{1}{\eta_7}\left(\frac{D\eta}{Dt}\right)_7 = -\frac{\omega_4}{\delta p}. \tag{75}$$

(The subscripts denote the level in hundreds of millibars.) Assuming that ω has a parabolic distribution between $p = 0$ and $p = 1000$ mb, we get $\omega_4 = \omega_6 = 0.96\ \omega_5$. But, as shown in the derivation of (29), ω_5 may be written

$$\omega_5 = \frac{1}{s}\left(\frac{D}{Dt}\right)_3 \ln(\phi_3 - \phi_7) = \frac{1}{s}\left(\frac{D}{Dt}\right)_7 \ln(\phi_3 - \phi_7). \tag{76}$$

Substitution in (75) then gives exactly (29), with ϕ_1 interpreted as ϕ_3 and ϕ_2 as ϕ_7. The quantity κ is now given by $-0.96\ (\delta p\, \partial \ln \theta/\partial p)^{-1} \approx 0.64\ \theta_5(\theta_3 - \theta_7)^{-1} \approx 8$. Thus, (71) to (74) apply to the 300- and 700-mb levels, if only ϕ' is defined as the 300-mb geopotential and ϕ as the 700-mb geopotential.

The lateral boundary conditions may be found by

the same heuristic reasoning as was used in NI for the barotropic model. Suppose ϕ' and ϕ are known functions of time on the boundary C of the simple closed region Γ. If q' and q were known at all times in the interior of Γ, we could solve the simultaneous system (73) and (74), which can be shown to have a unique solution, and so could determine ϕ' and ϕ as functions of time in the interior. But the physical equations (71) and (72) state that q' and q are advected with the fluid; if fluid is entering Γ at one level, say 700 mb, there is no way of knowing the associated value of q. Hence, q must be specified on C at those points where fluid is entering, *i.e.*, at those points where the tangential derivative of ϕ is positive in the direction which keeps the interior on the left. The same indeterminacy is not encountered where fluid is leaving. At such points, it is unnecessary to specify q' or q. Indeed, it is impossible to do so, for when fluid is leaving it carries its own q' or q with it.

The integration is carried out quite by analogy with the procedure B used for the integration of the barotropic vorticity equation. At time τ, we suppose that the quantities $q'^{\tau-1}$, q'^{τ}, $q^{\tau-1}$ and q^{τ} are stored. The difference analogues of (73) and (74),

$$\nabla^2\phi_{ij} = \frac{f_{ij}q_{ij}}{m_{ij}^2}[(\kappa+1)D - \kappa(\phi'_{ij} - \phi_{ij})] - \frac{f_{ij}^2}{m_{ij}^2}, \quad (77)$$

and

$$\nabla^2\phi'_{ij} = \frac{f_{ij}q'_{ij}}{m_{ij}^2}[\kappa(\phi'_{ij} - \phi_{ij}) - (\kappa-1)D] - \frac{f_{ij}^2}{m_{ij}^2}, \quad (78)$$

are then solved for ϕ' and ϕ, subject to the conditions that ϕ' and ϕ are given functions of time on the boundary. One may here assume that $\partial\phi'/\partial t = \partial\phi/\partial t = 0$ on the boundary, or else deal with the motion in a system rotating with constant angular velocity. In the latter case, it can be shown that there would be no appreciable change in q' or q, so that the transformation (70) for the boundary ϕ' or ϕ is all that would be required.

After ϕ'^{τ} and ϕ^{τ} have been determined, $(\partial q'/\partial t)^{\tau}$ and $(\partial q/\partial t)^{\tau}$ are evaluated from (71) and (72); and $q'^{\tau+1}_{ij}$ and $q^{\tau+1}_{ij}$ are calculated from the formulae

$$q'^{\tau+1}_{ij} = q'^{\tau-1}_{ij} + 2\,\Delta t\,(\partial q'/\partial t)^{\tau}_{ij}, \quad (79)$$

and

$$q^{\tau+1}_{ij} = q^{\tau-1}_{ij} + 2\,\Delta t\,(\partial q/\partial t)^{\tau}_{ij}. \quad (80)$$

Again, in the evaluation of the finite-difference Jacobian at points adjacent to the boundary, we invoke the boundary conditions in q' and q.

The principal problem is the solution of (77) and (78). Subtraction gives

$$\nabla^2_{ij}h - \frac{\kappa f_{ij}}{m_{ij}^2}(q'_{ij} + q_{ij})h_{ij} = -\frac{f_{ij}D}{m_{ij}^2}[(\kappa+1)q_{ij} + (\kappa-1)q'_{ij}], \quad (81)$$

where $h_{ij} = \phi'_{ij} - \phi_{ij}$. This is a difference analogue of a non-homogeneous self-adjoint linear partial differential equation of elliptic type, in the single variable h_{ij}. If it can be solved for $h_{ij} = \phi'_{ij} - \phi_{ij}$, substitution of $\phi'_{ij} - \phi_{ij}$ into (77) yields the difference analogue of a Poisson equation in the single variable ϕ_{ij}. Solving the latter for ϕ_{ij}, we obtain ϕ'_{ij} by adding ϕ_{ij} to $\phi'_{ij} - \phi_{ij}$.

It is proved in books on differential equations that (81), in continuous form, has a solution when the corresponding homogeneous equation does not. It can be shown that this will always be the case when $q' + q$ is positive, or negative but small. With the exception of certain small regions in the atmosphere, where the vorticity is strongly anticyclonic, both q' and q are positive, and even in these regions the η's are so little different from zero that $q' + q$ is sufficiently small. Hence, it is always possible to solve the system, (77) and (78). We remark that this is not so in the general baroclinic equation, from which (73) and (74) were derived by approximation. If the potential vorticity becomes negative, it can be shown that the three-dimensional potential vorticity equation in the height tendency becomes hyperbolic. In this case it is probable that no solution exists in the strict mathematical sense. However, in regions of negative potential vorticity it is likely that a kind of inertial instability sets in to reduce the potential vorticity to zero, just as static instability reduces the vertical potential-temperature gradient to zero. We may therefore be justified either in smoothing the negative potential vorticities to zero, or in assuming that the finite-difference equations — which *do* have a solution despite the existence of regions of negative q — govern the large-scale motions with sufficient accuracy.

With the definitions

$$\gamma_{ij} \equiv \kappa f_{ij}m_{ij}^{-2}(q'_{ij} + q_{ij})(\tfrac{1}{2}\,\Delta s)^2, \quad (82)$$

and

$$\mu_{ij} \equiv -f_{ij}m_{ij}^{-2}D[(\kappa+1)q_{ij} + (\kappa-1)q'_{ij}]\,\Delta s^2, \quad (83)$$

(81) becomes

$$\mathfrak{L}h_{ij} \equiv h_{i+1j} + h_{i-1j} + h_{ij+1} + h_{ij-1} - 4(1+\gamma_{ij})h_{ij} - \mu_{ij} = 0. \quad (84)$$

We may solve this equation by an extrapolated Liebmann process, exactly as we did the Poisson equation

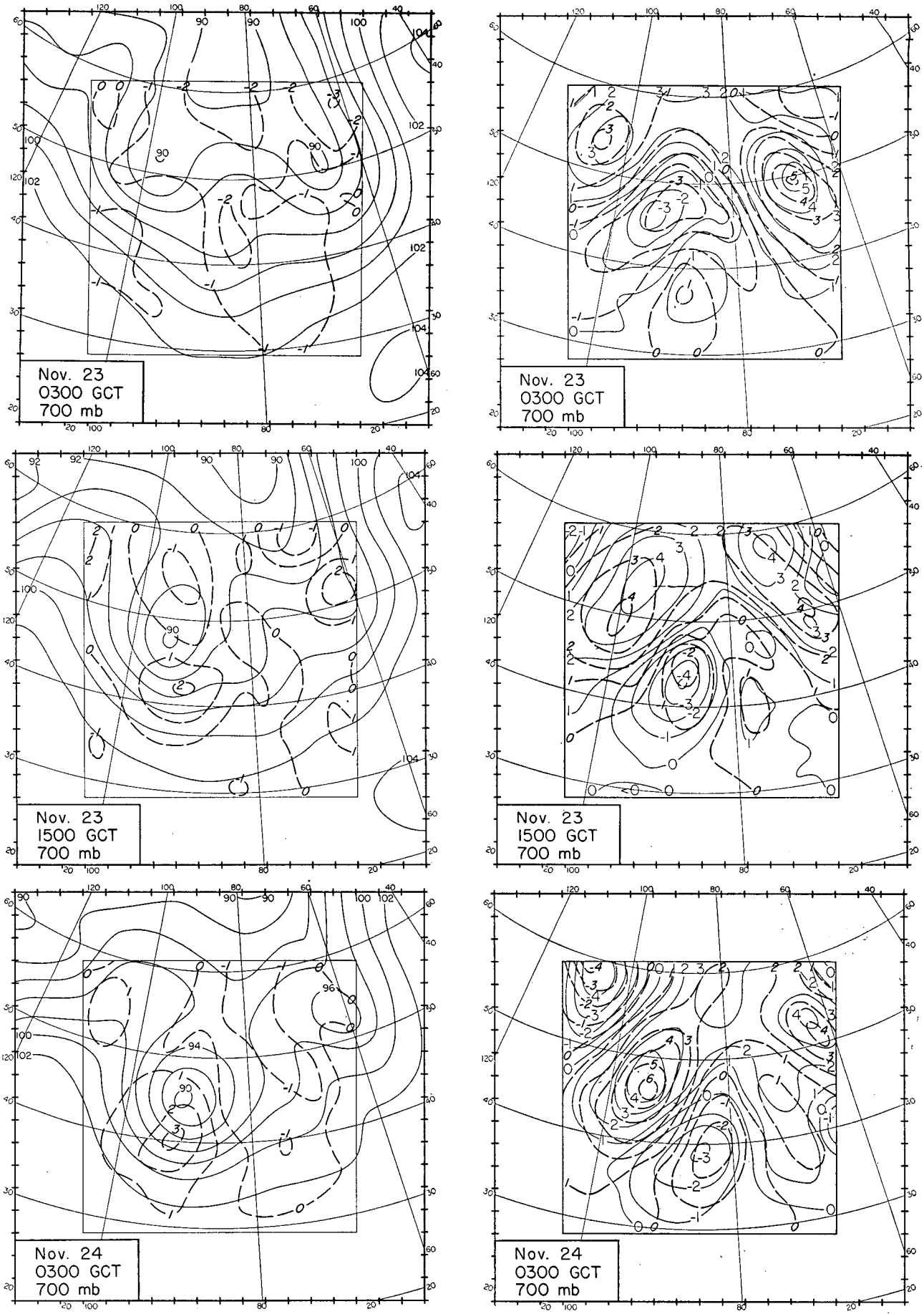

FIG. 6. 12-hr 2½-dimensional forecast data for 700 mb, November 1950. Left-hand charts contain initial 700-mb maps, with height contours (continuous lines) at 200-ft intervals and forecast errors (dashed lines) for 0300 GCT on 23rd (a, top), 1500 GCT on 23rd (b, center), and 0300 GCT on 24th (c, bottom). (Refer to fig. 4 for further explanation.)

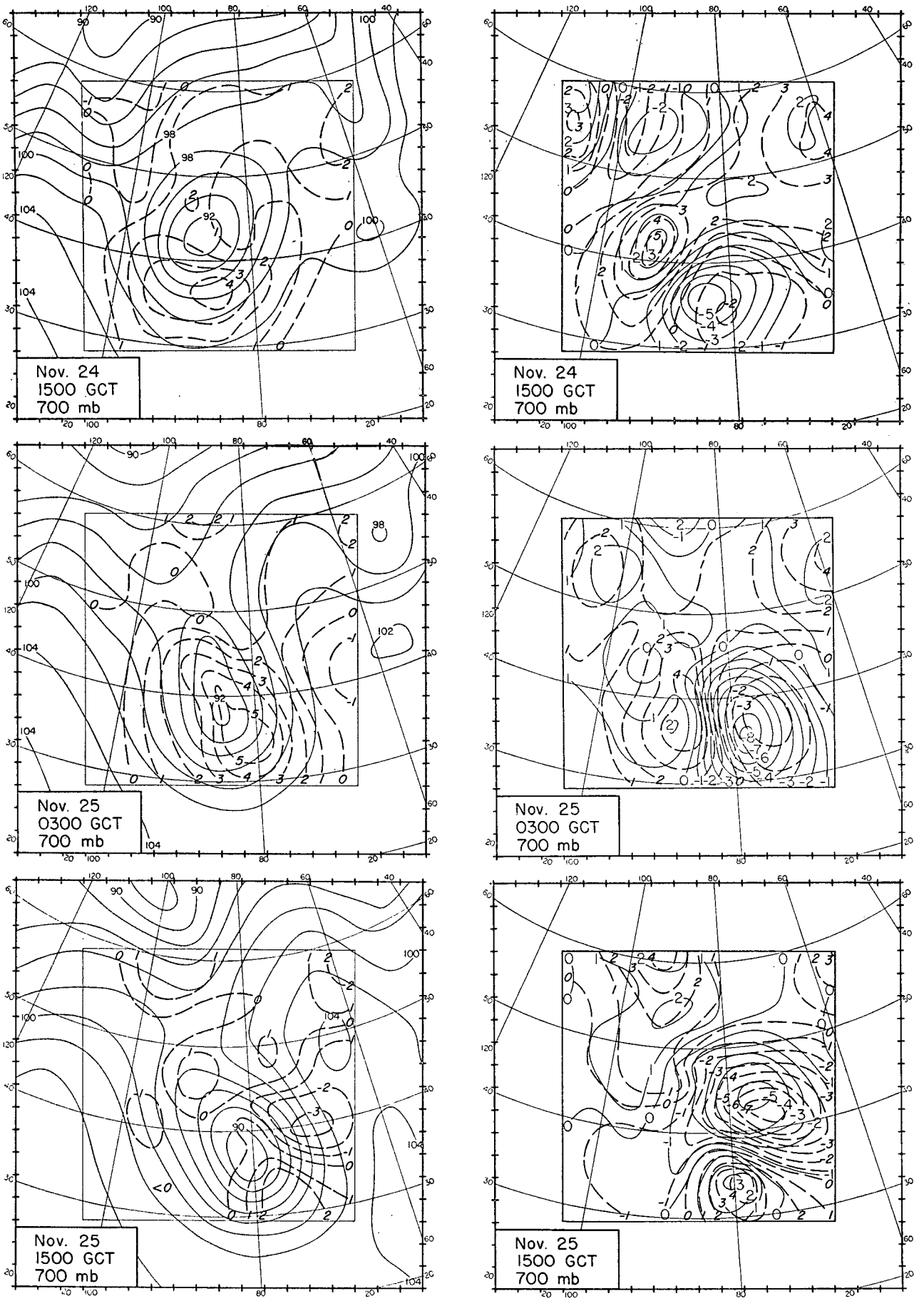

FIG. 7. 12-hr 2½-dimensional forecast data for 700 mb: (a, top), 1500 GCT 24 November 1950; (b, center), 0300 GCT 25 November 1950; (c, bottom), 1500 GCT 25 November 1950. (Refer to figs. 4 and 6 for further explanation.)

(51). By analogy with (54), we define the iteration process

$$h_{ij}^{\nu+1} = h_{ij}^{\nu} + \alpha \mathfrak{L} h_{ij}^{\nu,\nu+1}. \tag{85}$$

It is difficult to obtain the optimum α and exact convergence criteria, except when γ_{ij} is constant. In this case, setting $a = 1 + \bar{\gamma}_{ij}$, we can show by an adaptation of Frankel's (1950) method that the optimum α is $[2a(1+\sin\theta)]^{-1}$, where $\cos\theta = (2a)^{-1}(\cos\pi/p + \cos\pi/q)$, and that the maximum $|K_{rs}|$ is $4\alpha a - 1$. It was found experimentally that the α corresponding to the mean value of γ_{ij}, $\bar{\gamma}_{ij}$, gives as rapid convergence for the solution of (84) with variable γ_{ij} as with constant γ_{ij}. If a is appreciably greater than one, the convergence rate of the extrapolated Liebmann method is considerably better for (84) than for (54).

The computational stability criteria for the system (77) to (80) may be derived in a manner analogous to that used in NI for the barotropic vorticity equation. If terms that do not lead to an exponential amplification when $\Delta s \to 0$ are ignored, the stability criteria become

$$\Delta s/\Delta t > \sqrt{2}\,|v'|, \quad \Delta s/\Delta t > \sqrt{2}\,|v|, \tag{86}$$

where $|v'|$ is the maximum wind speed at 300 mb, and $|v|$ is the maximum at 700 mb. Thus, from the standpoint of computational stability, the difference analogues of (71) and (72) behave precisely as advection equations in which the velocity field is independent of the quantity being advected.

Because of the high particle velocities at 300 mb, it was necessary to take $\Delta t = \frac{1}{2}$ hr for $\Delta s = 300$ km; but to shorten the computation time, the accelerating scheme outlined earlier for the barotropic integration was used; the potential vorticities q' and q were advected in their respective velocity fields for three successive half-hour steps, and only then were the new ϕ' and ϕ computed by solving the difference analogues of (79) and (80) (the $3J/L$ process). Here, because of the small value of Δt, it was thought that the truncation errors introduced by using non-contemporaneous velocity fields would be small. As a check, a single 12-hr forecast was made in which ϕ' and ϕ were computed at every half-hour step (the $1J/L$ process). The differences between the 700-mb heights computed by the two methods are shown in fig. 2, together with the 12-hr height change computed by the $1J/L$ method. It will be seen that the differences are large. Unfortunately, this comparison was made only after all the forecasts had been completed and the diagrams drawn. The reader must therefore be asked to bear in mind that an appreciable truncation error is present in the $2\frac{1}{2}$-dimensional forecast diagrams (figs. 6 and 7). Just as in the barotropic forecast referred to previously, the error results from a too-great northward advection of the large cyclonic vorticities associated with a deep cyclone. Since it is observed from figs. 6 and 7 that the forecast errors also had this property, it appears that these errors would have been reduced had the $1J/L$ process been used throughout. Those forecasts in which the error was expected to be large were later recomputed with use of the $1J/L$ process (see next section).

A more accurate time-saving scheme would be to employ a procedure analogous to that recommended for the barotropic integration, namely to store the penultimate ϕ' and ϕ and extrapolate to obtain centered values for the Jacobian computation. With this scheme, it would not be necessary to use the same Δt at each level. q' and q could be advected separately, in time steps determined by the first and second of the criteria (86), respectively. It would, of course, be necessary to choose the time steps in the ratio of small whole numbers. Thus, one could advect q in one (or two) $1\frac{1}{2}$-hr steps and q' in three (or six) $\frac{1}{2}$-hr steps.

On the basis of the experience gained from the study of round-off error in the barotropic integrations, it was decided to allot twelve binary digits for the storage of ϕ^{τ}, and 14 binary digits each for the storage of q^{τ} and $q^{\tau-1}$ at each level. It was then possible to store all the data pertaining to one grid point as two forty-digit "words."

With use of the same horizontal grid dimensions as in the barotropic model, the length of time required to compute a 24-hr forecast was a little more than twice that for the barotropic model. Each $1\frac{1}{2}$-hr forecast involved the calculation of three fields of Jacobians for each level, and the solution by iteration of (81) and (77). With the machine operating at full speed, $1\frac{1}{2}$ min sufficed for the six Jacobian calculations, $2\frac{1}{2}$ min for the solution of (84), and $3\frac{1}{2}$ min for the solution of (77). Thus, a total time of 7 min per $1\frac{1}{2}$-hr time step, or 1 hr and 52 min per 24-hr forecast, was taken. This time can be considerably reduced by the use of procedures similar to those by which the barotropic forecast time was reduced from 48 to 6 min.

We remark, finally, that the number of multiplications performed and orders executed for each of the two Jacobian and Liebmann calculations was roughly the same as for the corresponding barotropic operations.

It is not necessary to solve the system (77) and (78) by reduction to an equation in a single dependent variable. The equations may be solved implicitly, by an extension of the extrapolated Liebmann method. We write them in the form

$$\begin{aligned} \mathcal{S}\phi_{ijk} \equiv \phi_{i+1jk} + \phi_{i-1jk} + \phi_{ij-1k} + \phi_{ij+1k} - 4\phi_{ijk} \\ + 4\gamma_{ijk}(\phi_{ij1} - \phi_{ij2}) + \mu_{ijk} = 0, \end{aligned} \tag{87}$$

where $\phi_{ij1} \equiv \phi'_{ij}$, $\phi_{ij2} \equiv \phi_{ij}$ $(k = 1, 2)$, and

$$\gamma_{ijk} = (-1)^k (\Delta s/2)^2 m_{ij}^{-2} f_{ij} q_{ijk},$$
$$\mu_{ijk} = (f \Delta s/m)_{ij}^2 - (f \Delta s^2/m^2)_{ij} q_{ijk}[1 + (-1)^k \kappa] D. \quad (88)$$

The iteration processes

$$\phi_{ijk}^{\nu+1} = \phi_{ijk}^{\nu} + \alpha \mathcal{S} \phi_{ijk}^{\nu,\nu+1}, \quad (89)$$

in which $\mathcal{S}\phi_{ijk}^{\nu,\nu+1}$ is defined in the same way as $\mathcal{R}\phi_{ij}^{\nu,\nu+1}$ in (54), can be shown to converge; and, in the case where the γ's and μ's are constant, to converge at essentially the same rate as the extrapolated Liebmann process (54) for the Poisson equation. This follows from the result that the eigenvalues for the operator $\mathcal{G}$ in the symbolic equation

$$\mathrm{E}^{\nu+1} = \mathcal{G}(\alpha)\, \mathrm{E}^{\nu}, \quad (90)$$

relating the errors $\mathrm{E}_{ij}^{\nu} = \phi_{ij}^{\nu} - \phi_{ij}$ and $\epsilon_{ij}^{\nu+1} = \phi_{ij}^{\nu+1} - \phi_{ij}$, consist of those for (54) and (85).[8]

Since integrations of the $[2 + (n-1)/n]$-dimensional model will eventually be made, it is appropriate to consider a possible integration program. As already pointed out, little appears to be lost if the system [(26), (27), (28)] is replaced by the simpler linearized system (34). This system may be written

$$\partial q_k/\partial t = J[f^{-1}(m^2 q_k + f^2), \phi_k], \quad (k = 1, 2, \cdots, n), \quad (91)$$

where

$$q_k = \nabla^2 \phi_k - f m^{-2}[\pi_k(\phi_k - \phi_{k+1}) - \pi_{k-1}(\phi_{k-1} - \phi_k)]. \quad (92)$$

A direct analogue of the method used for the $2\frac{1}{2}$-dimensional equations suggests itself here: Store the quantities q_k^{τ} and $q_k^{\tau-1}$; solve (92) for ϕ_k^{τ}; calculate $\partial q_k/\partial t$ from (91); and finally calculate $q_k^{\tau+1}$ from $q_k^{\tau+1} = q_k^{\tau-1} + 2\,\Delta t(\partial q_k/\partial t)^{\tau}$.

The extrapolated Liebmann process may be applied to solving (92) for all the ϕ_k's simultaneously, or to solving a transformed system each of whose equations contain but one dependent variable.

In the first case, we define

$$\mathfrak{M}\phi_{ijk} \equiv [\phi_{i+1j} + \phi_{i-1j} + \phi_{ij+1} + \phi_{ij-1} - 4\phi_{ij} - (\Delta s)^2 q_{ij}]_k - [f(\Delta s)^2 m^{-2}]_{ij}[\pi_k(\phi_{ijk} - \phi_{ijk+1}) - \pi_{k-1}(\phi_{ijk-1} - \phi_{ijk})], \quad (93)$$

and calculate ϕ_k from

$$\phi_{ijk}^{\nu+1} = \phi_{ijk}^{\nu} + \alpha \mathfrak{M}\phi_{ijk}^{\nu,\nu+1}. \quad (94)$$

It can be shown that the process converges. In the second case, we proceed as follows. We first assume that the factor $f(\Delta s)^2 m^{-2}$ may be absorbed in the π's, and the resultant quantities, π_k', treated as constant. The justification for this is the same as for replacing the absolute vorticity and the static stability by mean values, when they occur as factors. Equation (92) may then be written

$$\nabla^2 \phi_k + \sum_{s=1}^{n} A_{sk}\, \phi_s + C_k = 0, \ (k = 1, 2 \cdots, n), \quad (95)$$

where the matrix $A \equiv (A_{sk})$ is constant and symmetric. Let λ^r $(r = 1, 2, \cdots, n)$ denote its eigenvalues, defined as the n roots of the determinantal equation $|A - \lambda I| = 0$, where I is the unit matrix. Let $\psi_s{}^r$ $(s = 1, 2, \cdots, n)$ denote the components of the eigenvectors satisfying the equations

$$\sum_{k=1}^{n} A_{sk}\, \psi_k{}^r - \lambda^r \psi_s{}^r = 0, \quad (r, s = 1, \cdots, n). \quad (96)$$

Multiplying (95) by $\psi_k{}^r$, and summing over k, we obtain

$$\nabla^2 h_r + \lambda^r h_r + l_r = 0, \quad (97)$$

where

$$h_r = \sum_{k=1}^{n} \phi_k \psi_k{}^r; \quad l_r = \sum_{k=1}^{n} C_k \psi_k{}^r. \quad (98)$$

If the π's are all positive, as is the case here, it can be shown that the λ's are all negative, so that (97) is always soluble. The equations are solved singly, and the ϕ's are obtained from

$$\phi_s = \sum_{r=1}^{n} h_r \psi_r{}^s, \quad (s = 1, \cdots, n), \quad (99)$$

a relationship derived from the first of (98) by multiplication by $\psi_k{}^s$ and use of the orthogonality relationship

$$\sum_{r=1}^{n} \psi_r{}^s \psi_k{}^s = \begin{cases} 1, & r = k \\ 0, & r \neq k. \end{cases} \quad (100)$$

The equations (97) are of the same type as (81), and can be solved in the same manner by the extrapolated Liebmann method.

5. Discussion of results

The period selected for the forecasts was 0300 GCT 23 November to 1500 GCT 26 November 1950, and the forecast region the eastern part of the United States and southern Canada, an area with a relatively dense network of observing stations. It was decided that only for such an area was there a reasonable prospect of separating analysis errors from truncation and model errors. The uniform superiority of the *Eniac* forecasts for land areas, with good observational networks, over the forecasts for oceanic areas, with poor

[8] The writers are indebted to their associate, A. Nussbaum, for this result.

networks (NI), had already indicated the advisability of confining the experimental predictions to land and coastal areas. The eastern half of North America as a whole was also recommended because of its freedom from high mountain ranges, a complicating factor. The sequence of synoptic events that occurred during the period of the forecasts had already attracted wide attention as an unusually rapid and strong baroclinic development. It was felt that this sequence would provide an excellent laboratory in which to test the hierarchy of models.

The grid of points chosen for the forecast is shown in fig. 3. The region of validity for a 24-hr forecast is obtained by excluding a border strip, approximately three grid intervals in width.

Barotropic and baroclinic forecasts of 12 and 24 hr were prepared from each of the six initial maps: 0300 and 1500 GCT, 23, 24 and 25 November 1950. Each 24-hr forecast from an initial map overlapped the first half of the succeeding 24-hr forecast, with the exception, of course, of the last. Beginning at 0300 GCT 23 November, a relatively weak surface cyclone, centered near the western border of Lake Superior and containing an occluded front, drifted very slowly eastward and filled; 48 hr later it lay near the eastern border of Lake Superior. At that time the surface cyclone was quite weak, but the associated cold front, extending from the base of the occlusion in Ohio southwestward into the Gulf of Mexico and northward again through New Mexico, separated air masses of great density contrast. The associated upper cyclone at 500 mb was centered initially just west of Lake Winnipeg in Manitoba, and moved more rapidly but at a decelerating pace; by 1500 GCT November 24, it lay just over Chicago. At that time, a surface cyclone formed on the cold front, just south of the base of the occluded front, and deepened rapidly at the rate of about 1 mb/hr, so rapidly indeed that the winds after 24 hr had reached hurricane force along the Atlantic seaboard. An upper cyclone associated with the surface disturbance seemed to develop simultaneously, or just afterwards, and to amalgamate with the original cyclone aloft. The kinematic effect was a rapid acceleration of the original cyclone to the southeast. This process continued until 1500 GCT November 25, when the new surface cyclone reached its greatest development. Thereafter, the surface low-pressure center moved northwestwards, and the upper cyclone moved rapidly northwards for the first 12 hr and then stagnated.

The results of the six 12-hr barotropic forecasts for the 500-mb level are shown in figs. 4 and 5. The right-hand chart shows the observed and forecast height-changes, and the left-hand chart the initial map and the error map. The 12- and 24-hr computed displacements of the cyclone center are shown in fig. 8, in comparison with the observed displacements.

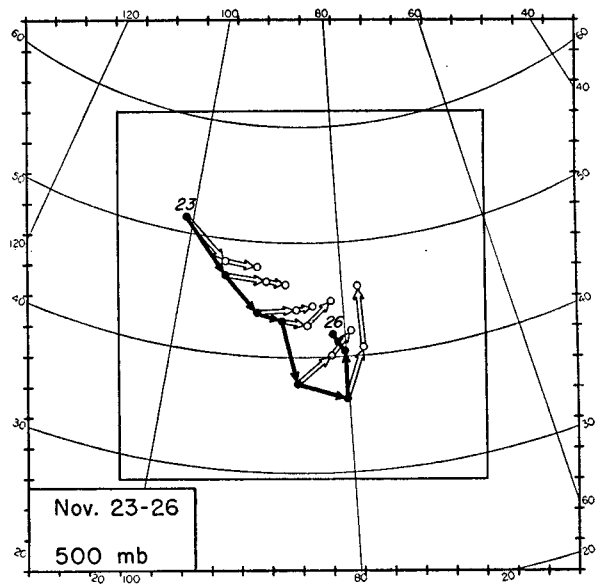

FIG. 8. Observed (solid arrows) and forecast (double-line arrows) trajectories of 500-mb height minimum. Positions shown at 12-hr intervals, beginning with 0300 GCT 23 November 1950.

The $2\frac{1}{2}$-dimensional 12- and 24-hr forecasts for 700 and 300 mb were prepared for the same periods as the barotropic forecasts. The results of the 700-mb forecasts are displayed in figs. 6 and 7. The observed and predicted changes are again shown on the right-hand charts, and the initial 700-mb charts, together with the forecast errors, on the left. The forecast 12- and

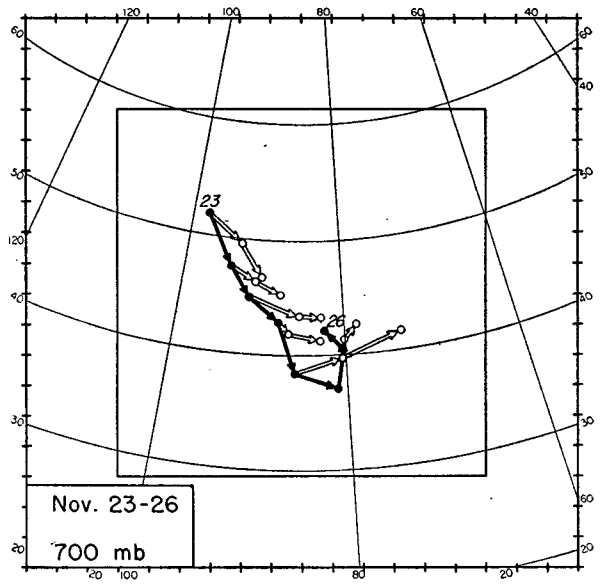

FIG. 9. Observed (solid arrows) and forecast (double-line arrows) trajectories of 700-mb height minimum. Positions shown at 12-hr intervals, beginning with 0300 GCT 23 November 1950.

24-hr displacements are shown in fig. 9, in comparison with the observed displacements.

The 24-hr forecast changes could not be shown for lack of space. However, correlation coefficients of the observed and computed changes, as well as root-mean-square deviations and root-mean-square observed changes, for both the barotropic 500-mb and the baroclinic 700-mb 12- and 24-hr forecasts, are given in table 1. Let x_i denote the deviation of an observed height change from its mean value over the region of validity of the forecast, and y_i the corresponding deviation of the forecast change. The correlation coefficient may then be written

$$r = \sum x_i y_i [\sum x_i^2 \sum y_i^2]^{-\frac{1}{2}},$$

and the root-mean-square deviation of y_i from x_i,

$$\bar{D} = [(169)^{-1} \sum (x_i - y_i)^2]^{\frac{1}{2}}.$$

The index i ranges over the 169 (13×13) grid points in the region of forecast validity (fig. 3). The quantity $\bar{D}$ is chosen as being more representative than the root-mean-square deviation of the predicted from the observed changes, because it is invariant with respect to an additive height-change field. The addition of a constant height-change alters neither dynamical quantities nor elements of weather. For comparison with $\bar{D}$, we also enter X and Y, the root-mean-square values of x_i and y_i, respectively:

$$X = (\sum x_i^2/169)^{\frac{1}{2}}, \quad Y = (\sum y_i^2/169)^{\frac{1}{2}}.$$

In the barotropic integrations, new vorticities and heights were computed every hour ($1J/L$). In the baroclinic integration, new potential vorticities were computed every $\frac{1}{2}$ hr, but new heights only every $1\frac{1}{2}$ hr ($3J/L$). In systems with strong winds and concentrated vorticities, the truncation error introduced in the latter integrations because of the non-centered ϕ is large, as shown in fig. 2. For the flow patterns investigated here, it can be shown, as remarked in an earlier section, that its effect is to produce too great a northward displacement of the cyclone during the period in which the winds were strongest and the vorticities most highly concentrated. [Compare figs. 2 and 7(b).] Accordingly the forecasts were recomputed by the $1J/L$ method for this period. On the average, the 12-hr correlation coefficients were increased by 7.5 per cent and the 24-hr ones by 4.5 per cent. Not all forecasts were so recomputed; quantities pertaining to those that were not are enclosed by parentheses in table 1.

It is evident that there is a consistent superiority of the $2\frac{1}{2}$-dimensional over the 2-dimensional forecasts, both for 12 and 24 hr. The superiority at 24 hr is the more marked. Here the baroclinic correlation coefficients average 11.5 per cent higher than the barotropic correlation coefficients, whereas at 12 hr they average only 5.8 per cent higher. Apparently the barotropic forecasts deteriorate more rapidly.

But perhaps the most noteworthy feature of the forecasts is their disagreement, rather than their agreement, with observation. Inspection of the forecast errors (figs. 4–7) reveals that the errors for the first 60 hr were due primarily to a failure to predict a fall in height south or southeast of the upper cyclone. A glance at the 700- and 500-mb charts for 1500 GCT 24 November [figs. 7(a) and 5(a)] shows almost complete agreement in phase, and the same bilateral symmetry about a NNE-SSW axis. Under such circumstances, neither the barotropic nor the $2\frac{1}{2}$-dimensional model can predict the observed southward displacement; the pressure rises and falls will be more or less symmetrically placed with respect to the axis of symmetry. Neither the advection of absolute vorticity by the wind, nor the advection of the nearly parallel field of thermal vorticity by the thermal wind, can produce the asymmetry needed. This is made most clear in fig. 10, which shows the potential vorticity field. The symmetrical arrangement of the potential vorticity field of the cyclone with respect to the wind field precludes the large southward displacement.

In an attempt to see if possibly the horizontal variation of static stability, which was ignored in the

TABLE 1. Correlation coefficients (r) and related statistical parameters X, Y and $\bar{D}$, for barotropic and $2\frac{1}{2}$-dimensional forecasts. X, Y and $\bar{D}$ in tens of feet. Figures in parentheses were obtained by $3J/L$ method.

	12 hour								24 hour							
	500 mb				700 mb				500 mb				700 mb			
Initial map	r	X	Y	$\bar{D}$	r	X	Y	$\bar{D}$	r	X	Y	$\bar{D}$	r	X	Y	$\bar{D}$
03 23 Nov	87	22	18	11	(89)	15	(15)	(7)	86	39	28	20	(90)	26	(27)	(12)
15 23 Nov	83	24	23	14	(86)	16	(14)	(8)	77	42	34	27	(87)	30	(24)	(14)
03 24 Nov	82	25	22	14	89	19	18	9	74	38	29	26	80	27	30	19
15 24 Nov	73	28	27	20	77	17	17	12	37	41	36	66	64	33	26	26
03 25 Nov	61	26	31	25	70	21	18	14	61	35.	36	32	56	28	27	26
15 25 Nov	78	21	28	17	(87)	16	(23)	(12)	60	29	39	32	(87)	21	(28)	(15)
Mean	77.3	24.3	24.8	16.8	83	17.3	17.5	10.3	65.8	37.3	33.7	33.8	77.3	27.5	27.0	18.7

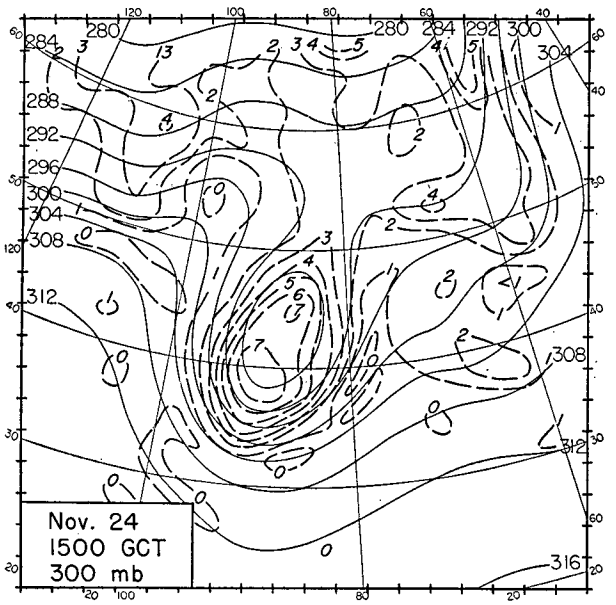

FIG. 10. 300-mb chart for 1500 GCT 24 November 1950, with height contours (continuous lines) at 200-ft intervals. Corresponding potential vorticity field is shown in dashed lines (in units of 10^{-8} sec^{-1} m^{-1}).

derivation of (26) and later of (29), could account for the discrepancy, the static stability measure κ was determined as a function of x and y and used in place of the constant mean value 8 [see text following (76)]. The observed κ chart is shown in fig. 11. The instantaneous change in the 700-mb height at 1500 GCT 24 November was evaluated from the system

$$\nabla^2\frac{\partial\phi_2}{\partial t} + J(\phi_2, \eta_2) + \frac{f\eta_2\kappa}{m^2(\phi_1 - \phi_2)} \times\left[\frac{\partial(\phi_1 - \phi_2)}{\partial t} + \frac{m^2}{f}J(\phi_2, \phi_1)\right] = 0, \quad (101)$$

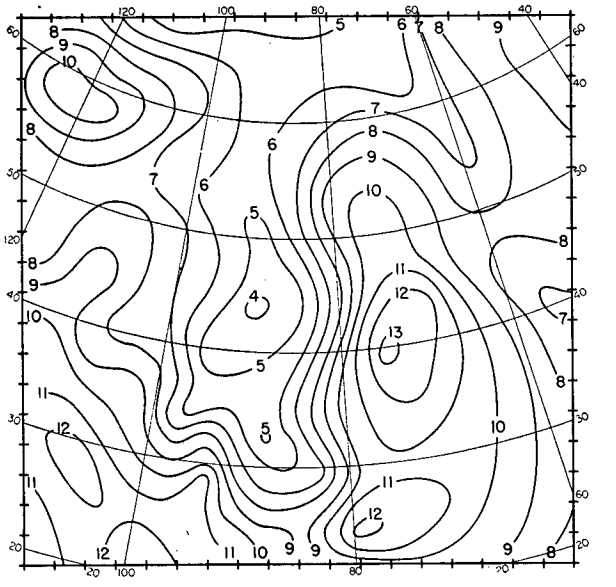

FIG. 11. Observed distribution of $\kappa \equiv 0.64\,\theta_5(\theta_3 - \theta_7)^{-1}$ at 1500 GCT 24 November 1950.

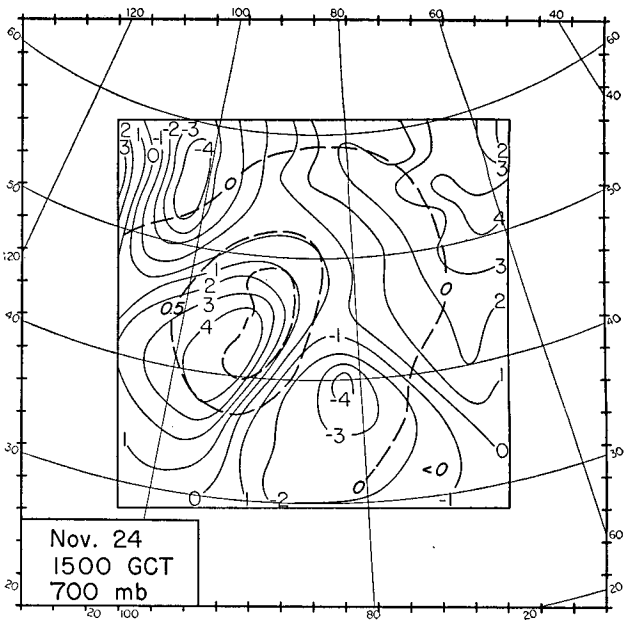

FIG. 12. Difference (dashed lines) between initial 700-mb height tendencies at 1500 GCT 24 November 1950, obtained with (a) variable stability factor $\kappa(x, y)$ shown in fig. 11 and (b) constant stability factor $\bar{\kappa} = 8$ [(a) − (b)]. Units are hundreds of feet per 12 hr. Solid lines are tendencies computed with $\bar{\kappa}$ (also hundreds of feet per 12 hr).

$$\nabla^2\frac{\partial\phi_1}{\partial t} + J(\phi_1, \eta_1) - \frac{f\eta_1\kappa}{m^2(\phi_1 - \phi_2)} \times\left[\frac{\partial(\phi_1 - \phi_2)}{\partial t} + \frac{m^2}{f}J(\phi_2, \phi_1)\right] = 0, \quad (102)$$

derived from (21). This change was compared with the corresponding change for constant mean κ. Fig. 12 shows the deviations of the former from the latter, compared with the latter. It will be seen, by comparison with the error chart in fig. 7(a), that the effect is small and does not account for the observed discrepancy.

It was postulated in the derivation of the system (34) that η could be replaced by a suitable constant $\bar{\eta}$. This assumption has been tested. The $2\frac{1}{2}$-dimensional equations derived from this approximation,

$$\left(\frac{D}{Dt}\right)_1\left[\eta_1 - \frac{\kappa\bar{\eta}}{D}(\phi_1 - \phi_2)\right] = 0, \quad (103)$$

and

$$\left(\frac{D}{Dt}\right)_2\left[\eta_2 + \frac{\kappa\bar{\eta}}{D}(\phi_1 - \phi_2)\right] = 0, \quad (104)$$

were integrated for 12 hr in $\frac{1}{2}$-hr time steps by the $3J/L$ process. The mean value of $\bar{\eta}$ was taken equal to f at 45°N. The deviation of these forecast 700-mb heights from those computed by means of (31) for the

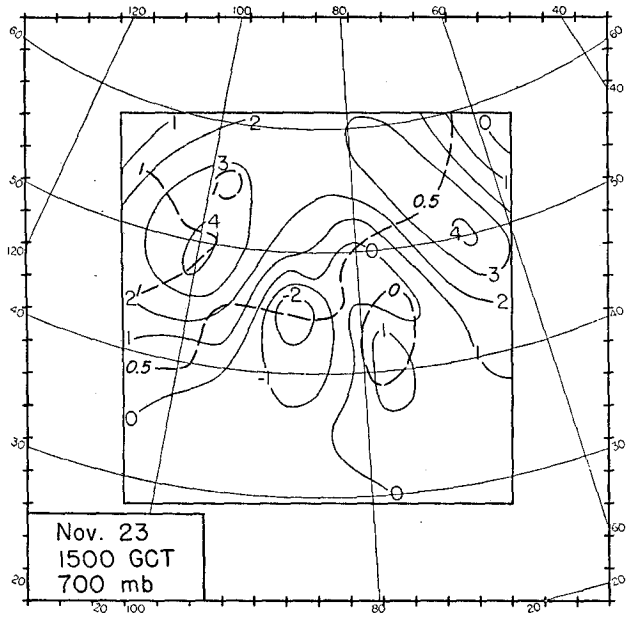

FIG. 13. Difference (dashed lines) in forecast 12-hr 700-mb height change (in hundreds of feet) obtained with (103), (104) and (31). Initial data taken at 1500 GCT 23 November 1950. 12-hr changes obtained from (31) are shown by continuous lines (in hundreds of feet).

same time steps are represented in fig. 13, together with the 12-hr changes computed from the latter equations. It is seen that the deviations are small.

Thus, it appears that the effects from the variations of the coefficients in the forecast equation are incapable of accounting for the observed forecast discrepancies. Moreover, because of the symmetry of the motion above the 700-mb level in the present instance, the wind — thermal wind interactions are also not responsible. The causes should therefore be sought in the low-level thermal asymmetries. Attempts might therefore be made to reformulate the $2\frac{1}{2}$-dimensional model, so as to take into account the low-level motions. This has actually been done, but with negative results. It seems likely, to the writers, that the difficulty is inherent in the basic crudity of a model in which the vertical structure of the atmospheric motion is given in terms of merely two parameters. This lack of definition is emphasized by the following considerations. Equation (16) relates the individual change of absolute vorticity at a given level to the individual expansion and contraction of isentropic unit layers. The change of the order of differentiation in passing to (18) may be interpreted as a statement that the individual expansion and contraction of an infinitesimal isentropic unit layer is proportional to the individual fluctuation of the potential-temperature difference between two infinitesimally separated isobaric surfaces. We now apply (18) to the 700-mb surface, and replace the infinitesimally separated isobaric surfaces by the 500- and 1000-mb surfaces, respectively. With the aid of the boundary condition (20), we arrive at the conclusion that the individual expansion and contraction of the isentropic surfaces at 700 mb can be replaced by the individual rate of change of potential temperature at 500 mb. This follows from the fact that the individual change of θ at the ground is effectively zero. When violent changes occur at low levels, as in the present case, the strong space- and time-fluctuations of *static stability* associated with the motion of the cold air-masses are obviously not reflected adequately in the potential-temperature fluctuations at 500 mb. More levels must be chosen to take into account the variations of static stability in a significant way. Three levels would permit horizontal individual changes of static stability. Four levels would also permit vertical variation, but this seems less important dynamically. Four levels is, however, the minimum number necessary to free the model of dynamical constraints not inherent in the geostrophic hypothesis.

The vertical velocity at 500 mb (w) can be obtained from the $2\frac{1}{2}$-dimensional forecast data in the following manner. Combining (1), (8) and the approximation

$$\omega \equiv dp/dt \approx w\,\partial p/\partial z,$$

we obtain the relation

$$w = -(100/64)(\kappa/g)(\partial/\partial t + \mathbf{v}\cdot\nabla)h, \qquad (105)$$

where $h = \phi_3 - \phi_7$, and $\mathbf{v}$ is either the 700-mb or 300-mb wind. Given h and ϕ_7, say, at times τ and $\tau - n$, $w^{\tau-\frac{1}{2}n}$ is given by

$$w^{\tau-\frac{1}{2}n} = -(100/64)\frac{\kappa}{g}\left[\frac{h^{\tau} - h^{\tau-n}}{n\,\Delta t} - \frac{m^2}{4f}J(h^{\tau} + h^{\tau-n}, \phi_7{}^{\tau} + \phi_7{}^{\tau-n})\right]. \qquad (106)$$

The values of w calculated from (106), with use of the forecast based on initial data at 0300 GCT 23 November, are shown in figs. 14, 15 and 16, together with surface fronts and weather observations. Fig. 14 was obtained with $\tau = 0$, $n = -6$; fig. 15 with $\tau = 24$, $n = 6$; and fig. 16 with $\tau = 48$, $n = 6$. It is suggested that the flow patterns in figs. 4 and 6 be kept in mind when interpreting figs. 14–16, since the attainment of saturation is more a function of the total vertical displacement undergone by a particle than a function of the instantaneous rate of ascent.

6. Solution of the general quasi-geostrophic equation

In this section, we outline a method for the solution of the quasi-geostrophic equations of motion for a general baroclinic atmosphere. The only assumptions, other than the trivial one of ignoring the horizontal

component of Coriolis force due to vertical motion, will be that the flow is adiabatic, quasi-static, quasi-geostrophic and frictionless.

In the coordinate system x, y, p, t, the basic equation of motion may be obtained from (3), (1), (7) and (8). After some rearrangement of terms, we obtain the following equation for $\partial\phi/\partial t$:

$$[\nabla^2 + (f\eta/m^2e)(\partial^2/\partial p^2 + a\,\partial/\partial p)]\,\partial\phi/\partial t = b, \quad (107)$$

in which

$$\begin{aligned} e &= (\partial\phi/\partial p)\,\partial \ln\theta/\partial p = p^{-1}(c_v/c_p)\,\partial\phi/\partial p + \partial^2\phi/\partial p^2, \\ a &= -(\eta e)\,\partial(\eta e)/\partial p, \\ b &= J(\eta, \phi) + e^{-1}\eta(a + \partial/\partial p)\,J(\partial\phi/\partial p, \phi). \end{aligned} \quad (108)$$

The boundary condition at the top of the atmosphere ($p = 0$) is strictly that $\omega \equiv dp/dt = 0$. But because the initial motion is not known at pressures less than about 100 mb, and because influences from above 100 mb cannot be expected to affect the low-level motions within one or two days (Charney, 1949), we are justified in imposing an artificial, though physically possible and therefore mathematically consistent, boundary condition. One might, for example, treat the 100-mb surface as a free surface. In this case, the boundary condition becomes $\omega = 0$ at $p = 100$, or, by (1), (6) and (8),

$$[\partial(\partial\phi/\partial t)/\partial p]_{100\text{ mb}} = f^{-1}m^2\,J(\partial\phi/\partial p, \phi)_{100\text{ mb}}. \quad (109)$$

For the lower boundary condition, we use the same device as for the $[2 + (n-1)/n]$-dimensional model, except that here we permit the ground to vary in elevation. Defining $\varpi(x, y)$ as the standard-atmosphere pressure at the ground, we require the three-dimensional flow to be parallel to the surface $p = \varpi(x, y)$ instead of the ground. Since the slope of this surface will always differ negligibly from the slope of the ground, the error introduced will be quite small. The mathematical form of the boundary condition is derived from the adiabatic equation, and becomes

$$\frac{1}{(\partial\phi/\partial p)_\varpi}\left[\frac{\partial}{\partial p}\left(\frac{\partial\phi}{\partial t}\right)\right]_\varpi = \frac{m^2}{f}J\left[\frac{c_v}{c_p}\ln\varpi + \ln\left(\frac{\partial\phi}{\partial p}\right)_\varpi, \phi\right]_\varpi, \quad (110)$$

where the subscript ϖ denotes evaluation at $p = \varpi(x, y)$.

The lateral boundary condition is obtained by the same type of reasoning as used for the simpler models. Here it is the potential vorticity, $\eta\,\partial \ln\theta/\partial p$ that moves with the fluid. Supposing first that ϕ is prescribed on the boundary for all time, we find that the potential vorticity must be prescribed where fluid is entering but must not be prescribed where fluid is leaving. Since $\partial \ln\theta/\partial p$ on the boundary is obtainable from ϕ on the boundary, it is only necessary to specify η or $\nabla^2\phi$ at inflow points.

The difference analogue of (107) can be solved for $\partial\phi/\partial t$, by an extension of the extrapolated Liebmann process. In a manner analogous to procedure A, section 3, the quantities ϕ^τ and $\phi^{\tau-1}$ would be stored in the machine at the beginning of the process, and after $(\partial\phi/\partial t)^\tau$ is determined, $\phi^{\tau+1}$ would be found from $\phi^{\tau+1} = \phi^{\tau-1} + 2\,\Delta t\,(\partial\phi/\partial t)^\tau$. The quantities η/e, a and b could be recomputed as needed in the iteration process, or else computed before-hand and stored. In the former case, the computation time would be very great, and in the latter the storage requirements would be unconscionably large. Altogether, the use of either of these methods is not recommended.

An alternative method, analogous to procedure B, section 3, would be to let the potential vorticity q carry the history of the motion and determine ϕ as needed, from a solution of the equation

$$(f^{-1}m^2\,\nabla^2\phi + f)[p^{-1}(c_v/c_p) + (\partial\phi/\partial p)^{-1}(\partial^2\phi/\partial p^2)] = q, \quad (111)$$

assuming it were possible. However, the time integration of q by the conservation law,

$$\partial q/\partial t = -\boldsymbol{v}\cdot\nabla q - \omega\,\partial q/\partial p, \quad (112)$$

involves the storage of the auxiliary quantity ω. This

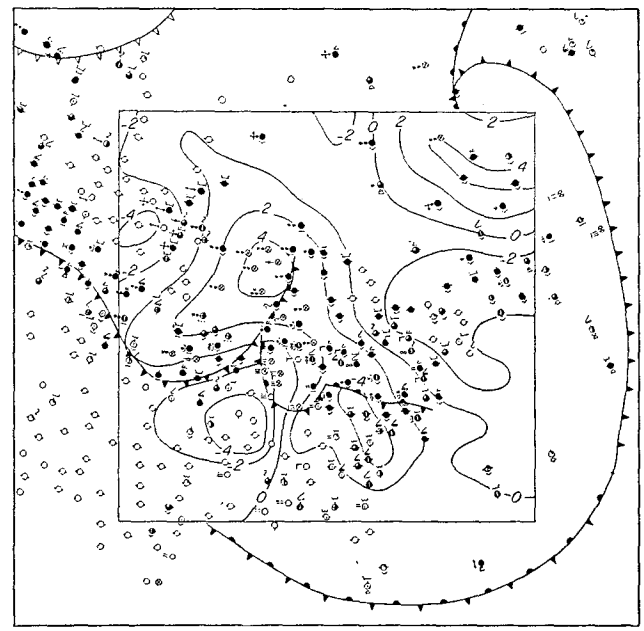

FIG. 14. Vertical velocities (cm/sec) from 2½-dimensional model, at 0430 GCT 23 November 1950, as forecast from initial data at 0300 GCT. Also shown are surface frontal locations and weather observations at 0630 GCT.

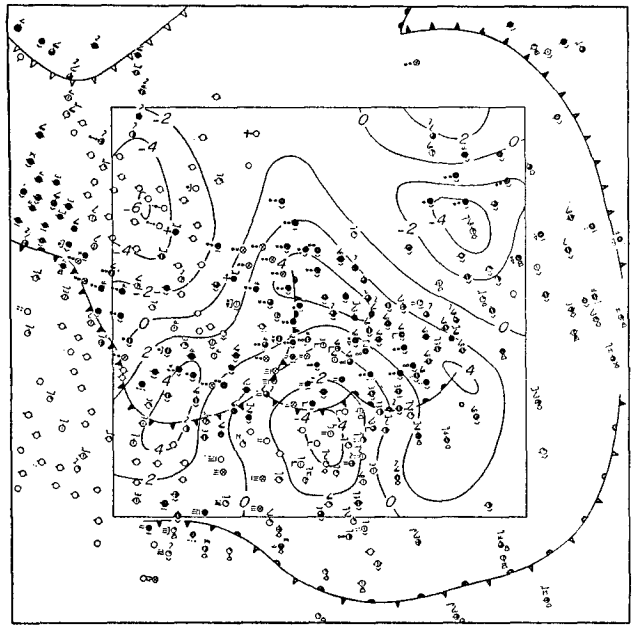

FIG. 15. Vertical velocities (cm/sec) from 2½-dimensional model, at 1330 GCT 23 November 1950, as forecast from initial data at 0300 GCT. Also shown are surface frontal locations and weather observations at 1230 GCT.

quantity would have to be calculated from (1) and (8), but this requires a contemporaneous value of $\partial\phi/\partial t$. To calculate $(\partial\phi/\partial t)^\tau$ as a centered difference, one would have to know $\phi^{\tau+1}$, which, of course, is not known until *after* the time extrapolation of q. Hence, a non-centered $\partial\phi/\partial t$, and therefore a non-contemporaneous ω, would have to be used. If $(\partial\phi/\partial t)^\tau$ were approximated by $(\phi^\tau - \phi^{\tau-1})/\Delta t$, it can be shown that the computation would be unstable. Hence, more sophisticated and complicated methods must be used. The storage requirements would again become formidable. Hence this method is not recommended.

If centered space- and time-differences are used in the solution of (111), the computational stability is essentially determined by the simple advection equation (112). The same heuristic type of argument used in NI leads to the following computational stability criterion:

$$\Delta s/\Delta t > (\sqrt{2m}\,|v| + (\Delta s/\Delta p)\,|\omega|)_{\max},$$

where Δp is the vertical increment in p. Writing $\delta p = |\omega\,\Delta t|_{\max}$, we obtain

$$\Delta s/\Delta t > \sqrt{2m}\,|v|_{\max}\,(1 - \delta p/\Delta p)^{-1}.$$

For any reasonable choice of the increments Δs, Δt and Δp, it can be shown that $\delta p/\Delta p \ll 1$. Hence, the stability does not depend significantly on Δp; and Δs and Δt should be chosen to satisfy the relation $\Delta s/\Delta t > \sqrt{2m}\,|v|_{\max}$, just as in the case of the simpler models.

The computational difficulties arising in the x, y, p, t coordinate system are also present in the x, y, z, t system. They are not, however, present in the semi-Lagrangian system x, y, θ, t. This is because the potential vorticity is advected along a coordinate surface (θ = constant). Shuman (1951) has discussed some advantages of the θ system for the quasi-geostrophic model.

We introduce the Montgomery stream-function (the "isentropic acceleration potential") Ψ:

$$\Psi = c_pT + \phi, \tag{113}$$

where T, the absolute temperature, and ϕ, the geopotential, are now regarded as functions of x, y, θ and t. The hydrostatic and geostrophic relationships take the forms

$$\partial\Psi/\partial\theta = c_pT/\theta, \tag{114}$$

and

$$v = f^{-1}k \times \nabla\Psi, \tag{115}$$

respectively. (Unless otherwise stated, all differentiations with respect to x, y or t, here and in what follows, are to be carried out at constant θ.)

The potential vorticity q may be defined by

$$q \equiv -(f + \zeta)(\partial p/\partial\theta)^{-1}, \tag{116}$$

where $\zeta = \partial v/\partial x - \partial u/\partial y$, and the equation for the conservation of potential vorticity is

$$\frac{dq}{dt} = \frac{\partial q}{\partial t} + v\cdot\nabla q = \frac{\partial q}{\partial t} - \frac{m^2}{f}J(q, \Psi) = 0. \tag{117}$$

In the derivation of this equation, only the conventional assumptions of adiabatic, non-viscous and hydrostatic flow are involved. The quantity $\partial p/\partial\theta$ in (116) is readily expressed in terms of Ψ, by means of the perfect-gas equation and (114):

$$\partial p/\partial\theta = \text{constant} \times (\partial\Psi/\partial\theta)^{2.5}(\partial^2\Psi/\partial\theta^2). \tag{118}$$

[Here we have set $c_v/(c_p - c_v) = 2.5$.] Substituting this expression into (116), and introducing the geostrophic assumption (115), we obtain

$$q = -(f^{-1}m^2\,\nabla^2\Psi + f) \div [(\partial\Psi/\partial\theta)^{2.5}(\partial^2\Psi/\partial\theta^2)]. \tag{119}$$

The first factor in the above equation is normally positive, and the last is normally negative; hence, q is normally positive. If q is supposed known as a function of x, y and θ, Ψ can be obtained by solving the equation[9]

$$\nabla^2\Psi + m^{-2}fq(\partial\Psi/\partial\theta)^{2.5}(\partial^2\Psi/\partial\theta^2) + (f/m)^2 = 0. \tag{120}$$

Since q is normally positive, this will ordinarily be an

[9] Kleinschmidt (1950) has used essentially this same method to deduce the flow patterns corresponding to simple prescribed distributions of q.

elliptic equation in the highest derivatives. The occurrence of the non-linear term $(\partial\Psi/\partial\theta)^{2.5}$ should give no trouble. (It may even be approximated as a standard function of θ.) Schematically, (120) may be solved as follows. We first define a difference analogue for the lattice points $x = i\,\Delta s$, $y = j\,\Delta s$, $\theta = k\,\Delta\theta$ ($i = 0, 1, \cdots, p$; $j = 0, 1, \cdots, q$; $k = 0, 1, \cdots, r$):

$$\mathcal{P}\Psi_{ijk} \equiv \Psi_{i+1jk} + \Psi_{i-1jk} + \Psi_{ij+1k} + \Psi_{ij-1k} - 4\Psi_{ijk} + \left(\frac{f\,\Delta s^2}{m^2}\right)_{ij} q_{ijk} \left(\frac{\Psi_{ijk+1} - \Psi_{ijk-1}}{2\,\Delta\theta}\right)^{2.5} \times \left(\frac{\Psi_{ijk+1} + \Psi_{ijk-1} - 2\Psi_{ijk}}{(\Delta\theta)^2}\right) + \left(\frac{\Delta s\, f}{m}\right)^2_{ij} = 0. \tag{121}$$

An extrapolated "Liebmann" iterative process is defined by

$$\Psi^{\nu+1}_{ijk} = \Psi^{\nu}_{ijk} + \alpha\mathcal{P}\Psi^{\nu,\nu+1}_{ijk},$$

where it is assumed that the points are scanned in lexicographic order with k first, j second, and i third. It has been shown (Young, 1951) that the process converges for certain boundary conditions when the continuous equation is elliptic, and, of course, in the absence of the non-linear factor. While no rigorous proof of convergence can be given in the present case, there is no apparent reason why the process should not succeed here also. It is probable that the continuous equation has no solution compatible with the physically determined boundary conditions when q is not greater than or equal to zero everywhere in the domain of integration. Nevertheless, it is expected that the small "hyperbolic" regions in the atmosphere will create no difficulty in the solution of the *difference* equations, for the reason stated in connection with the discussion of (81).

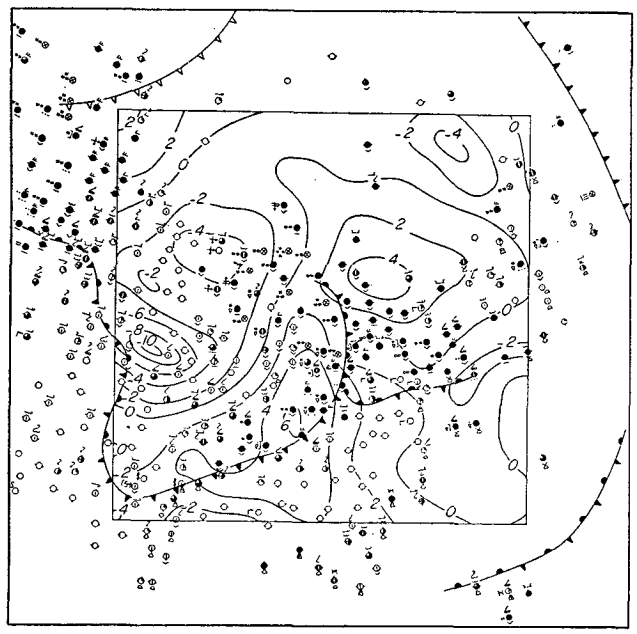

FIG. 16. Vertical velocities (cm/sec) from 2½-dimensional model, at 0130 GCT 24 November 1950, as forecast from initial data at 0300 GCT 23 November. Also shown are surface frontal locations and weather observations at 0030 GCT 24 November.

The boundary condition at the ground most suitable for our present purpose is obtained from (113) and (114). Setting $\phi = \phi_0(x, y)$ and $\theta = \theta_0(x, y, t)$ at the ground, we have simply

$$(\Psi - c_pT)_{\theta=\theta_0} = (\Psi - \theta\,\partial\Psi/\partial\theta)_{\theta=\theta_0} = \phi_0(x, y). \tag{122}$$

It is also necessary to know how θ_0 varies. It can be shown that its variation is given by

$$\partial\theta_0/\partial t = f^{-1}m^2\,J(\theta_0, \Psi_0), \tag{123}$$

where Ψ_0 is the stream function at the ground.

For the upper boundary condition, it is convenient to assume that a sufficiently elevated isentropic surface is fixed in space. The condition is then identical to (122), except that $\phi_0(x, y)$ is replaced by $\phi_\mu(x, y)$, the geopotential of the upper rigid surface:

$$(\Psi - \theta\,\partial\Psi/\partial\theta)_{\theta=\theta_\mu} = \phi_\mu(x, y). \tag{124}$$

Since the surface is isentropic, a counterpart equation to (123) is not needed.

The lateral boundary condition is derived as in the previous cases. With Ψ a given function of time on the lateral boundaries, q must be specified at inflow points but not at outflow points. The computational stability criterion is again given by $\Delta s/\Delta t > \sqrt{2}\,|v|_{\max}$, as in the (x, y, p, t)-system.

We solve the system (121) and the difference analogue of (117) by an obvious extension of procedure B. With the quantities ϕ_μ, ϕ_0, $\theta_0^{\tau-1}$, θ_0^{τ}, $\Psi^{\tau-1}$, q^{τ} and $q^{\tau-1}$ stored at time τ, we calculate Ψ^{τ} from (121), making use of the boundary conditions (122) and (123) in difference form, and the given values of Ψ on the lateral boundary. $(\partial q/\partial t)^{\tau}$ is then calculated from the difference analogue of (117), with use of the lateral boundary condition on q, *i.e.*, the treatment of inflow and outflow points on the lateral boundaries will be the same as that for the simpler models. $q^{\tau+1}$ is obtained from $q^{\tau-1}$ and $(\partial q/\partial t)^{\tau}$, by centered time extrapolation. $(\partial\theta_0/\partial t)^{\tau}$ is evaluated from the difference form of (123), and $\theta_0^{\tau+1}$ is determined from $\theta_0^{\tau-1}$ and $(\partial\theta_0/\partial t)^{\tau}$ by centered time extrapolation. We see that the method requires the storage of the two quantities $\theta_0^{\tau-1}$ and θ_0^{τ} at the lower-boundary grid points, in addition to ϕ_0 and ϕ_μ.

It is necessary to devote some attention to the proper selection of the vertical grid interval. An obvious choice would be a constant $\Delta\theta$. However, this may not be the best choice. The problem may be formulated as follows. Given the ability to store data representing, say, N levels, what is the "most efficient"

placement for these levels? — that is to say — how should they be placed so as to reduce truncation error to a minimum? The elliptic nature of (121) when $q > 0$ means that, although the solution Ψ at any one point A depends on the q values everywhere within the region of integration, it depends most strongly on the q values nearest A. [This has been shown graphically by Hinkelmann *et al* (1952) for a modified form of (107), and is also implicit in Charney's (1949) discussion of the vertical propagation of influences by the linearized form of (107).] This would imply that the levels should be closest together at those heights for which a forecast is most desired, *e.g.*, the lower troposphere. Furthermore, the initial data are less accurate at high levels than at lower elevations, so that a very accurate representation of the observations at high levels would be partly superfluous.

The quality and density of the aerological network in North America suggests that it would be reasonable to set the upper boundary of the forecast region in the vicinity of $\theta = 400\text{K}$ ($p \approx 100$ mb). The selection of a constant $\Delta\theta$ would then result in almost twice as many levels above the tropopause as below! A more reasonable location of the vertical grid points can be obtained, however, if one replaces the vertical coordinate θ by

$$\chi \equiv \theta^{-n}. \tag{125}$$

For $n \approx 10$, it can be shown that equal increments in χ correspond approximately to equal pressure intervals. The selection of constant $\Delta\chi$ for the vertical mesh is, therefore, more in agreement with the considerations in the preceding paragraph. The substitution $\chi = \theta^{-n}$ produces only a trivial modification in the basic equations (119), (122) and (123). Equation (117) remains unaltered.

Although the transformation $\theta \rightarrow \chi$ gives a reasonable spacing of lattice points in the vertical, it does not eliminate one of the basic difficulties inherent in the use of the system x, y, θ, t. This difficulty is that the lower boundary of the region, the surface of the earth, is not fixed in the θ or χ system. This difficulty is present in the p system also, but has been overcome there by the device of replacing the actual surface pressure $p_0(x, y, t)$ by a standard surface pressure $p = \varpi(x, y)$. This cannot be done in the θ or χ system, since the surface potential temperature at a given point may vary within 24 hr by almost as much as the potential temperature difference between the ground and tropopause! Although this is not an insurmountable obstacle, it means that much extra code and computation time are required to provide sufficient flexibility in the storage of data at the grid points. Furthermore, along the verticals with low surface potential-temperature, there would be perhaps twice as many grid points at which data was stored as along verticals with high surface potential-temperature.

The extremely simple system [(117), (121), (122), (123), (124)] has evidently been obtained at the expense of complicating the storage of data and the treatment of the lower boundary. Since the difficulty arises from the fact that the ground is not a fixed surface in the χ system, the difficulty may be partly overcome by transforming the χ system to one in which the ground is a coordinate surface. Since the earth's surface has no simple mathematical properties, it can be expected that the equation of motion will become more complicated. However, we may avoid the complication to some extent by *solving* the equations in the χ system and *storing* the data in a new coordinate system, obtained by introducing the vertical coordinate

$$\sigma \equiv (\chi - \chi_0)(\chi_\mu - \chi_0)^{-1},$$

where χ_0 denotes the surface χ and χ_μ the (constant) value of χ at the upper rigid χ-surface corresponding to $\theta = 400\text{K}$. We see that σ varies between 0 and 1, and takes on the limiting values at the ground and at the upper boundary, respectively. Thus, the ground becomes a coordinate surface, and the upper boundary remains a coordinate surface.

The boundary conditions (122) and (124) remain essentially the same; we need only the transformation

$$\theta \frac{\partial}{\partial\theta} = \theta \frac{\partial\chi}{\partial\theta}\frac{\partial\sigma}{\partial\chi}\frac{\partial}{\partial\sigma} = \frac{n\chi}{\chi_0 - \chi_\mu}\frac{\partial}{\partial\sigma}.$$

The equation for the variation of χ_0, (123), remains exactly as before.

In the computation, the q's and Ψ's are stored at the grid points in the σ system: $x = i\,\Delta s$, $y = j\,\Delta s$, $\sigma = k\,\Delta\sigma$. [$i = 0, 1, \cdots, p$; $j = 0, 1, \cdots, q$; $k = 0, 1, \cdots, r = (\Delta\sigma)^{-1}$.] The computations involved in (117) and (121) are then carried out in the χ system, the required values of q and Ψ being derived by interpolation from the stored values in the σ system.

We remark finally that thermal and surface frictional effects may be taken into account without seriously complicating the numerical calculations. If we no longer assume that the motion is adiabatic, and denote the individual rate of change of potential temperature by Q, it may easily be shown [for example, as a consequence of Ertel's (1942) general form of the potential vorticity theorem] that the potential vorticity becomes, with small approximation,

$$\frac{dq}{dt} = q\frac{\partial Q}{\partial\theta} + \frac{q}{f+\zeta}\nabla\frac{\partial v}{\partial\theta} \times \nabla Q \cdot \boldsymbol{k}, \tag{126}$$

where

$$d/dt = \partial/\partial t + \boldsymbol{v}\cdot\nabla + Q\,\partial/\partial\theta. \tag{127}$$

On the assumption that the heating function Q has a

horizontal scale comparable to that of the motion itself, one may show that the second term on the right is small compared with the first. Hence, we obtain

$$\frac{\partial q}{\partial t} = \frac{m^2}{f} J(q, \Psi) + q \frac{\partial Q}{\partial \theta} - Q \frac{\partial q}{\partial \theta}, \qquad (128)$$

in place of (117). The equation corresponding to (123) is then

$$\frac{\partial \theta_0}{\partial t} = \frac{m^2}{f} J(\theta_0, \Psi_0) + Q_0, \qquad (129)$$

where Q_0 is the surface value of Q.

Surface friction may be introduced in the manner suggested by Charney and Eliassen (1949). The frictionally produced convergence in the friction layer gives rise to a vertical velocity at the top of the friction layer which, on the Ekman theory, depends only on the surface geostrophic velocity. We therefore replace the surface boundary condition (122) by

$$\frac{d\phi}{dt} = \left(\frac{\partial}{\partial t} + v \cdot \nabla + Q_0 \frac{\partial}{\partial \theta}\right)\left(\Psi - \theta \frac{\partial \Psi}{\partial \theta}\right) = g w_0, \qquad (130)$$

where

$$g w_0 \approx v_0 \cdot \nabla \phi_0 + g(K/2f)^{\frac{1}{2}} \sin 2\alpha \, \zeta_0. \qquad (131)$$

Here ζ_0 is the surface vertical vorticity component, K the "eddy diffusivity," and α is the angle between the isobars and the surface wind. Combining (130) and (131), we obtain, with small approximation,

$$\frac{\partial}{\partial t}\left(\Psi - \theta \frac{\partial \Psi}{\partial \theta}\right) = \frac{m^2}{f} J\left(\Psi - \theta \frac{\partial \Psi}{\partial \theta} - \phi_0, \Psi\right) - \theta Q_0 \left(\frac{\partial^2 \Psi}{\partial \theta^2}\right)_0 - g(K/2f)^{\frac{1}{2}} (\sin 2\alpha) \left[\left(\frac{\partial \Psi}{\partial \theta}\right)^{5/2} \frac{\partial^2 \Psi}{\partial \theta^2} q - f\right], \qquad (132)$$

at the top of the friction layer, say 500 m above the ground.

An alternative method of introducing the effect of surface friction may be to add to (128) at the ground level a term proportional to $k \cdot \nabla \times F$, where F is the effective frictional force in the surface layers. The lower boundary condition on Ψ would then be simply (122). This procedure would have the advantage of not requiring past values of Ψ in the vicinity of the ground, whereas (132) requires this information.

Acknowledgments.—The writers wish particularly to acknowledge their indebtedness to Prof. J. von Neumann, for many valuable suggestions concerning methods of integration of the meteorological equations. They also wish to express their thanks to Mr. G. Lewis for coding the integrations, to Dr. J. Smagorinsky, Dr. B. Gilchrist and Mrs. N. Gilbarg for help in performing the computations, to Mr. E. Hovmöller for analyzing the weather charts used in the integrations, to the staff of the Electronic Computer Project at the Institute for Advanced Study for their interest and patience in carrying out the lengthy and involved computations, and to the Dept. of Meteorology, University of Chicago, and Mrs. D. Friedlander for the drafting of the figures.

REFERENCES

Bolin, B., and J. Charney, 1951: Numerical tendency computations from the barotropic vorticity equation. *Tellus*, **3**, 248–257.

Charney, J. G., 1948: On the scale of atmospheric motions. *Geofys. Publ.*, **17**, No. 2, 17 pp.

——, 1949: On a physical basis for numerical prediction of large-scale motions in the atmosphere. *J. Meteor.*, **6**, 371–385.

——, and A. Eliassen, 1949: A numerical method for predicting the perturbations of the middle latitude westerlies. *Tellus*, **1**, No. 2, 38–54.

Charney, J. G., R. Fjørtoft, and J. von Neumann, 1950: Numerical integration of the barotropic vorticity equation. *Tellus*, **2**, 237–254.

Craig, R. A., 1945: A solution of the nonlinear vorticity equation for atmospheric motion. *J. Meteor.*, **2**, 173–178.

Eady, E. T., 1952: Note on weather computing and the so-called $2\frac{1}{2}$-dimensional model. *Tellus*, **4**, 157–167.

Eliassen, A., 1949: The quasi-static equations of motion with pressure as independent variable. *Geofys. Publ.*, **17**, No. 3, 44 pp.

——, 1952: Simplified dynamic models of the atmosphere, designed for the purpose of numerical prediction. *Tellus*, **4**, 145–156.

Ertel, H., 1942: Ein neuer hydrodynamischer Wirbelsatz. *Meteor. Z.*, **59**, 277–281.

Fjørtoft, R., 1951: Stability properties of large-scale atmospheric disturbances. *Compendium of meteorology*. Boston, Amer. meteor. Soc., 454–463.

——, 1952: On a numerical method of integrating the barotropic vorticity equation. *Tellus*, **4**, 179–194.

Frankel, S. P., 1950: Convergence rates of iterative treatments of partial differential equations. *Math. tables and other aids to computation*, **4**, No. 30, 65–75.

Hinkelmann, K., O. Essenwanger, G. Reymann, and F. Wippermann, 1952: Physikalisch-mathematische Grundlagen der numerischen Integration in einer baroklinen Atmosphäre. *Ber. Deut. Wetterd. U.S.-Zone*, No. 38, 416–428.

Høiland, E., 1950: On horizontal motion in a rotating fluid. *Geofys. Publ.*, **17**, No. 10, 26 pp.

Kleinschmidt, E., 1950: Ueber Aufbau und Entstehung von Zyklonen. *Meteor. Rund.*, **3**, 1–6.

Neamtam, S. M., 1946: The motion of harmonic waves in the atmosphere. *J. Meteor.*, **3**, 53–56.

Phillips, N. A., 1951: A simple three-dimensional model for the study of large-scale extratropical flow patterns. *J. Meteor.*, **8**, 381–394.

Platzman, G. W., 1952: Some remarks on high-speed automatic computers and their use in meteorology. *Tellus*, **4**, 168–178.

Richardson, L. F., 1910: The approximate arithmetical solution by finite differences of physical problems involving differential equations, with an application to the stresses in a

masonry dam. *Phil. Trans. roy. Soc. London*, A, **210**, 307–357.

Rossby, C.-G., 1940: Planetary flow patterns in the atmosphere. *Supplement, Quart. J. r. meteor. Soc.*, **66**, 68–87.

Shuman, F. G., 1951: *Solutions of a differential equation of pressure tendency.* Technical Rpt. No. 9, Research on atmospheric pressure change, Dept. Meteor., Mass. Inst. Tech., 135 pp.

Southwell, R. V., 1946: *Relaxation methods in theoretical physics.* Oxford, Clarendon Press, 248 pp.

Sutcliffe, R. C., 1947: A contribution to the problem of development. *Quart. J. r. meteor. Soc.*, **73**, 370–383.

Thompson, P. D., 1948: The propagation of permanent-type waves in horizontal flow. *J. Meteor.*, **5**, 166–168.

Young, D., 1951: *Iterative methods for solving partial difference equations of elliptic type.* Seminar given at Numerical Analysis Seminar of Ballistic Research Laboratories, Aberdeen Proving Ground, Md. (Based on Ph.D. thesis by author, Harvard Univ., Cambridge, Mass., 1950.)